From blackness to invisibility – carbon nanotubes role in the attenuation of and shielding from radio waves for *stealth* technology

Anna Kolanowska[1], Dawid Janas[1], Artur P. Herman[1], Rafał G. Jędrysiak[1], Tomasz Giżewski[2,*], Sławomir Boncel[1,*]

[1] Silesian University of Technology, Department of Organic Chemistry, Bioorganic Chemistry and Biotechnology, Krzywoustego 4, 44-100 Gliwice, Poland

[2] Lublin University of Technology, Faculty of Electrical Engineering and Computer Science, Nadbystrzycka 38A, Lublin, Poland

*corresponding authors; tel. +48 32 237 12 72; fax +48 32 237 20 94; e-mail: slawomir.boncel@polsl.pl (S. Boncel); tel. +48 81 538 42 94; t.gizewski@pollub.pl (T. Giżewski)

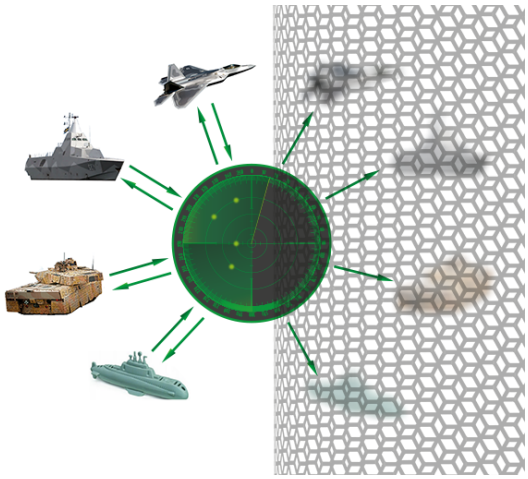

Abstract

Stealth technology combines numerous means and techniques to be 'invisible' for opponents in a battle field. Since metals are the key construction materials of military vehicles, weapon and equipment, they can be targeted and detected by RAdio Detection And Ranging (RADAR) systems. Radar-Absorbent Materials (RAMs) – as crucial components of passive countermeasures in the modern-day military tactics – are used for absorption of electromagnetic waves. In the same time, mainly due to high electric conductivity, RAMs – accompanied by designed geometry of the objects they are incorporated into – can yield programmable reflection, multiple internal reflection and scattering towards Electromagnetic

Interference (EMI) shielding. Nowadays, the latest achievements of nanotechnology have transformed *stealth* technology into an even more powerful tool. And among many nanomaterials, carbon nanotubes (CNTs) have arisen as one of the most promising active component of RAMs and EMI shielding materials. The unique sp^2-derived macromolecular architecture equips CNTs with an exceptional combination of electromagnetic, mechanical and chemical properties. This review intends to summarize and critically evaluate the hitherto efforts in the production and applications of CNT nanocomposites/hybrid materials as key constructional civil and military elements, preferably as coatings, layers, films, textiles or panels, towards attenuation of the radio wave radiation.

1. Introduction

Stealth technology, also known as low observable technology, has recently emerged as a crucial passive countermeasure in military tactics. Use of various carbon forms, mostly as Radar Absorbing Materials (RAMs), is not a new idea – it dates back to 1936 in Netherlands. The first patent concerning RAM – realized in a constructional approach – was an absorber of a quarter-wave resonant type using carbon black (CB) as a lossy resistive material and TiO_2 for high permittivity (ε) to reduce the overall thickness [1]. In 1944 wings of a German bomber Horten Ho 229 (also called Gotha Go 229) were made from CB-impregnated plywood glued together with a mixture of charcoal and sawdust. In parallel, Germans used graphite particles dispersed in a rubber matrix, next to ordinary paper, in a three-layer material called *Sumpf* (Eng. 'swamp') and *Schornsteinfeger* (Eng. 'chimney-sweeper'). Application of this composite has allowed for reduction of reflectivity of radio waves in the submarine periscopes [2]. Autonomously, Americans have applied a similar solution but they replaced graphite with CB to obtain Halpern Anti-Radiation Paint (HARP) used in the aircrafts [3]. The dielectric matrix of HARP had elevated relative permittivity (150 F m^{-1}) due to loading with oriented disk-shaped aluminium flakes and CB for reflection losses – both suspended in a rubber matrix. Today after 80 years and after searching for 'carbon AND radar absorbing material', Google yields 205,000 while Espacenet® 246 hits, respectively.

In the 'battlefield' of *stealth* technology itself, development of RAMs accompanied a continuous advance in the construction of increasingly sophisticated radars as a natural counteraction. In principle, all radars constitute systems exploiting microwaves (MW) to detect, locate and determine velocity of the objects and can work in a high range of transmitted frequencies depending on the operational conditions. MW-transmitter emits

focused waves of a length from 1 mm up to tens of meters and the corresponding frequency from 300 GHz to 50 MHz (**Fig. 1**).

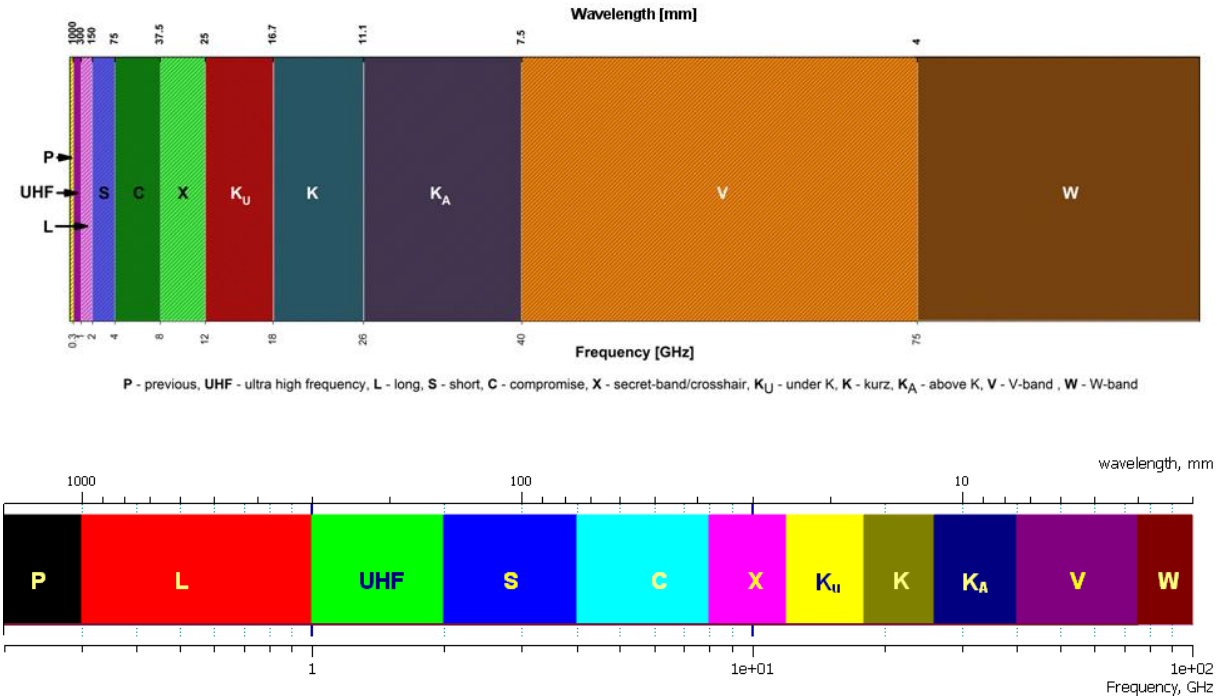

Fig. 1 Radar frequency bands with their origins of abbreviation (UHF – ballistic missile early warning, L – air traffic control, S – weather radar, C – transponder, X – marine and airport radar, K_u – satellite transponders, K – weather and photo radar, K_a – photo radar): in linear (*above*) and logarithmic (*below*) scales; **the colours from the linear scale** will be consequently applied throughout the paper in order to **identify EM-wavelengths** at glance

The higher frequency of radar the more it is affected by weather conditions such as rain, fog, humidity or clouds. On the other hand, higher frequencies offer more precise accuracy of the analysis. Generally, once the EM radiation encounters in its path an object of dielectric or diamagnetic constant different from that of the medium in which it moves – the radiation is reflected, absorbed, dispersed or transmitted. This behaviour depends on radiation wavelength and a parameter called Radar Cross Section (RCS) which evaluates how detectable by radar an object is. The magnitude of RCS depends on the target itself (size, shape, surface smoothness and other material parameters it is made of, etc.) and the parameters of the radar beam (incident/reflected angle, wavelength, polarization, etc.) (**Fig. 2**).

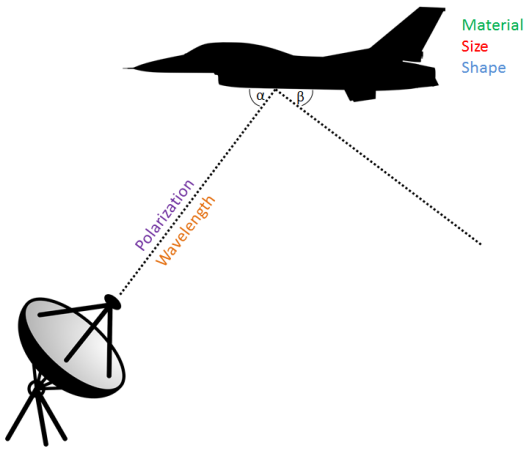

Fig. 2 A simplified selection of the most important parameters influencing RCS of a given object

Radiation is reflected particularly strongly by materials of high electrical conductivity. If the wavelength is much shorter than the object, a mirror image is obtained. In turn, if the wavelength is much longer, the reflection is so weak that the object is 'imperceptible' by the radar. One can be hence claimed that 'detectability' of the object results from the resonance associated with a comparable wavelength and size of the object. This phenomenon allows for registering the object by radar. Furthermore, a use of dual linear polarization (vertical and horizontal) allows for a significant improvement in the identification accuracy of the reflecting surface. More sophisticated approaches such as application of circular polarization enable to eliminate the influence of rain droplets and other weather conditions.

RAMs are typically multi-component (mainly layered) composites and/or hybrid materials of a convenient spatial arrangement with a tunable response against MWs. Apart from absorption of radiation emitted by the radar transmitters, RAMs are designed to minimize the backscatter. Also, as MW absorption corroborates with generation of heat, the evolved thermal energy must be dissipated in the *stealth* systems in order to prevent from detection by thermal signature. Other critical properties which RAMs shall display are: strong absorption coefficient over a wide range of MW frequencies, light weight, straightforward production and the expedient final macro-assembling [4]. It is nonetheless simply unattainable to find all of the above properties in the individual material. Metallic conductors are heavy, expensive and prone to corrosion. On the other hand, typical lightweight polymers are insulators. Hence, the required complexity can be realized by compounding electrical conductors with a portion of ferromagnetic and dielectric components while the matrices could be composed from common lightweight and processable polymers [5].

Nanotechnology has opened up the possibility of radical enhancement of RAMs. Heavy and corroding fillers are tested to be gradually swapped for lightweight conducting polymers or sp^2-carbon allotropes such as CNTs or graphene. A significant impact of the carbon filler type and its dimensionality – and therefore conductivity – could be demonstrated by a fact that the same Shielding Effectiveness (*SE*) is achievable by a content of 10 wt.% of CB, 5 wt.% of carbon nanofibres and only 1 wt.% of multi-wall CNTs (MWCNTs) [6]. Apart from those excellent and tunable electrical properties (by selection of the nanotube chirality or doping), CNTs display other unique combination of desirable physicochemical properties such as high thermal conductivity or impressive mechanical performance [7] which are definitely critical for the *stealth* technology.

According to our best knowledge, there is a gap in the systematic overview of applications of CNTs in the *stealth* technology. For example, Saville et al. have compiled a theory of anti-radiolocation, but only mentioned about the *stealth* constructive materials [8]. The more comprehensive approach was published by Vinoy and co-workers, wherein the authors discussed theory of EM absorption, though, abstracting from the materials site again [9]. One of the first reviews including materials considerations was nevertheless deprived of information about CNTs because they were at the early stage of development at that time [10]. An important input of Geetha et al. – published 12 years later – was focused on conductive polymers with excellent anti-radiolocation properties, but the progress on this front in carbon nanomaterials was again insufficiently mature to be included in this work [11]. It is then evident that while – or maybe rather because of – the subject was extensively explored by the military science and technology [12,13], the idea has been neglected for a moment in the review literature. The only reviews showing the potential of carbon-related materials were published earlier in 2001 [14] and in 2012 by Saini and Arora [15], with the latter showing only a rather partial view at CNTs as RAM components.

Taking all the above into consideration, we present the up-to-date review on CNT-based materials to be potentially applied in the *stealth* technology. Radar absorbing properties, accompanied typically by EMI shielding, were evaluated in the context of CNT morphology, content, exohedral versus endohedral chemistry, 3D-arrangement of macro- and micro-assemblies and/or compatibility with a variety of matrices. This approach intends to reveal the full potential of CNTs and their functionalized counterparts as active components in the scalable RAMs and EMI shielding composites.

2. Electromagnetic waves at the boundary of materials – premises for *stealth* technology

To consider the mechanism of radar devices, one must recall the classic electromagnetism theory generated from the Maxwell equations in the complex form (**Eq. 1**), where **r** represents the vector of distance from antenna source to the object, $\underline{\mathbf{E}}$ and $\underline{\mathbf{H}}$ are electric and magnetic field intensity, respectively, $\underline{\mathbf{J}}$ - total current density, $\mu(\mathbf{r})$ – tensor form of the permeability, $\varepsilon(\mathbf{r})$ - tensor form of permittivity, f – frequency, and i – imaginary unit.

$$\begin{cases} \nabla\left(\varepsilon(\mathbf{r})\cdot\underline{\mathbf{E}}(\mathbf{r},t)\right)=\rho(\mathbf{r}) & (\mathrm{a}) \\ \nabla\left(\mu(\mathbf{r})\cdot\underline{\mathbf{H}}(\mathbf{r},t)\right)=0 & (\mathrm{b}) \\ \nabla\times\underline{\mathbf{H}}(\mathbf{r},t)=\mathrm{i}2\pi f\,\underline{\mathbf{D}}+\underline{\mathbf{J}}(\mathbf{r}) & (\mathrm{c}) \\ \nabla\times\underline{\mathbf{E}}(\mathbf{r},t)=-\mathrm{i}2\pi f\mu(\mathbf{r})\underline{\mathbf{H}}(\mathbf{r}) & (\mathrm{d}) \end{cases} \qquad \textbf{(Eq. 1)}$$

The inner area of the object is characterized by the function on the right side of the equation (**Eq. 1a**) and, for the objects devoid of the electric charge, equals $\rho(\mathbf{r})=0$. The equation (**Eq. 1c**) describes the magnetic field in the area containing a current source (i.e. displacement and/or conductive current). The simplification to the linear and homogeneous medium as well as plane wave in dielectric areas ($\underline{\mathbf{J}}(\mathbf{r})=\underline{\mathbf{J}}=0$) yields a phase shift between the magnetic and electric components. Hence, in order to describe the conductive area, the wave amplitude is dampened, according to the equation (**Eq. 2**), with the real solution for the plane waves in the time domain (**Eq. 3**).

$$\nabla^2\underline{\mathbf{E}}+\omega^2\mu\left(\varepsilon-\frac{\mathrm{i}\sigma}{\omega}\right)\underline{\mathbf{E}}=0 \qquad \textbf{(Eq. 2)}$$

$$\mathbf{E}(\mathbf{r},t)=\mathrm{Re}\left(\mathbf{E}_0 e^{\mathrm{i}(\underline{k}r-\omega t)}\right) \qquad \textbf{(Eq. 3)}$$

where wave number k is defined with formula (**Eq. 4**).

$$\underline{k}^2=\mu\varepsilon\omega^2+\mathrm{i}\mu\sigma\omega \qquad \textbf{(Eq. 4)}$$

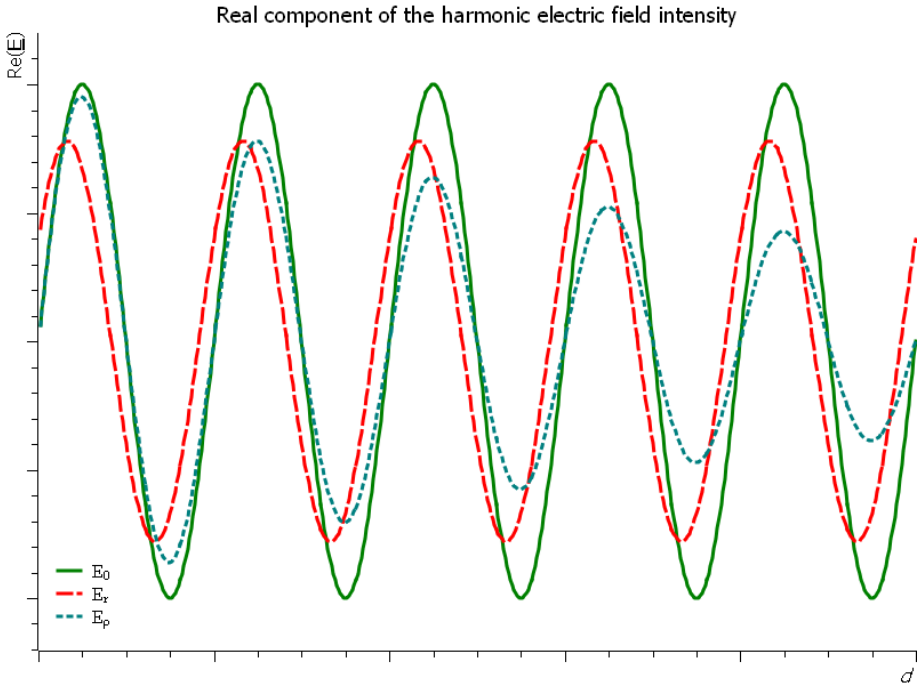

Fig. 3 The real part distribution of the electric component: E_0 – derives from the source, E_r – reflected and, E_p – absorbed wave in the homogeneous conductive medium

At the boundary of two regions with different values of permeability and permittivity, the electrical and magnetic components are changed according to the general boundary conditions (**Eq. 5**), where E_{1n}, E_{2n} are normal components of the electric field intensity vector and E_{1t}, E_{2t} are tangential components of the electric field intensity vector; in the same time H_{1n}, H_{2n} are normal components of the magnetic field vector and H_{1t}, H_{2t} are tangential components of the magnetic field vector.

$$\begin{cases} \varepsilon_1 E_{1n} = \varepsilon_2 E_{2n} \\ E_{1t} = E_{2t} \\ \mu_1 H_{1n} = \mu_2 H_{1n} \\ H_{1t} = H_{2t} \end{cases} \qquad \textbf{(Eq. 5)}$$

The analysis of the equations (**Eq. 2**) at the boundary of regions (**Eq. 5**) proves that the electromagnetic wave is reflected and absorbed (dispersed in the conductive region) and the phase and magnitude are changed (**Fig. 3**). The above simple considerations allow to the determine the properties of the reflected signal as a result of the energy balance.

The total energy dw stored in the volume dV in the electric field and the magnetic field is given by (**Eq. 6**). The surface density of total energy **S** is described with the Poynting vector presented in (**Eq. 7**).

$$\mathrm{d}w = \left(w_{\mathrm{E}} + w_{\mathrm{H}}\right)A(\mathbf{r})\mathrm{d}\mathbf{r} = \frac{1}{2}\left(\varepsilon(\mathbf{r})\mathbf{E}^2(\mathbf{r}) + \mu(\mathbf{r})\mathbf{H}^2(\mathbf{r})\right)A(\mathbf{r})\mathrm{d}\mathbf{r} \qquad \textbf{(Eq. 6)}$$

$$\mathbf{S} = \mathbf{E} \times \mathbf{H} \qquad \textbf{(Eq. 7)}$$

Radar antennae are typically capacitive sensors and hence, due to its importance, one must analyse the electrical component of the EM-wave as dominant. The voltage signal on the output is the averaged value induced as the effect of the incident electric field.

3. Mechanisms describing shielding properties

The losses of electromagnetic radiation power result from the following phenomena: (1) reflection, (2) absorption and/or (3) multiple reflections (**Fig. 4**). As mentioned earlier, for a given wave frequency, the sum of all losses is called shielding effectiveness (*SE*). It is expressed in dB units and defined by logarithm of the ratios (**Eq. 8**) and, referring to the formula (**Eq. 6**), the relationship can be represented as a function of the electric field or magnetic field intensity [16].

$$SE = 10\log\left(\frac{P_{\mathrm{in}}}{P_{\mathrm{em}}}\right) = 10\log\left(\frac{E_{\mathrm{in}}^2}{E_{\mathrm{em}}^2}\right) = 20\log\left(\frac{E_{\mathrm{in}}}{E_{\mathrm{em}}}\right) \qquad \text{(Eq. 8)}$$

where:

P_{in} – intensity of the incident radiation, W sr^{-1}

P_{em} – intensity of the emitted radiation, W sr^{-1}

E_{in}, H_{in} – intensity of electric/magnetic field incident radiation, V m^{-1} (N C^{-1}); A m^{-1}

E_{em}, H_{em} – intensity of electric/magnetic field emitted by a cover, V m^{-1} (N C^{-1}); A m^{-1}

Clearly, as concerning constructions for the *stealth* solutions, one must here emphasize that reflections of incident radiation should be re-directed carefully in order to avoid just a simple return of the wave back to the receiver. On the other hand, the reflected signal should be comparable with the background in order not to generate similarly suspicious ‘black hole’ in the scanned area.

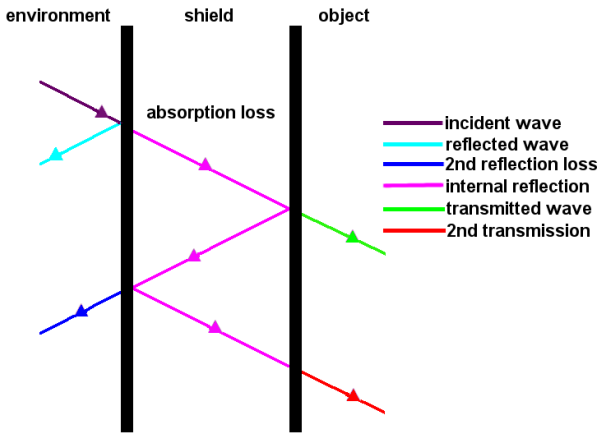

Fig. 4 A schematic view into the principle phenomena of EMI shielding by perfectly smooth surfaces

As said, when an electromagnetic wave encounters a barrier, a wave transmitted beyond this barrier is changed in phase and magnitude by reflection, multiple internal reflections and absorption. The radiation meets the material in a way that its portion is reflected, whereas the remainder penetrates the interior. The reflection losses occur at the interfaces between the transmitting (or surrounding) medium and the shielding material, and result from the mismatch in the wave impedance between the medium and the material. Reflection is associated with the difference of the materials wave impedance and the presence of mobile (free) charge carriers (electrons, 'holes') interacting with the radiation. In turn, absorption occurs as the wave passes through the conductive material. The absorption losses in the energy of electromagnetic wave result from dissipated heat generated by eddy currents induced in the material by magnetic fields of the travelling wave – according to the Joule-Lenz Law [17]. The recorded decrease in intensity is related to the finite conductivity of the material (see **Eq. 3**) and polarization of the atoms and molecules. Absorption requires conductive regions or the presence of electric and magnetic dipoles interacting with electric and magnetic field. The electric and magnetic dipoles are provided by the materials of high permittivity (ε) and permeability (μ), respectively [18].

Both reflection losses (SE_R) (**Eq. 9**) and absorption losses (SE_A) (**Eq. 10**) are proportionally dependent on electrical conductivity. Both types of losses are related to permeability of the material and frequency of radiation, but reflection is directly while absorption inversely dependent on those variables. In turn, absorption is permittivity independent [19].

$$SE_R = -10\log\left(\frac{\sigma}{16\varepsilon\omega\mu}\right) \qquad \textbf{(Eq. 9)}$$

$$SE_{\mathrm{A}} = -8.68d \log\left(\frac{\sigma\omega\mu}{2}\right) \qquad \textbf{(Eq. 10)}$$

where:

d – thickness of material, m

It is now clear that high electrical conductivity, low permittivity and low permeability generate high reflectance, whereas in order to achieve high absorbance – high electrical conductivity and high permeability are required. Moreover, SE_A increases proportionally with a thickness of material (d) and hence a compromise between weight and performance of the constructed object must be attained. Although a change in SE_{A} would be more pronounced than SE_{R} by a change in electrical conductivity, in total, shielding by materials of high electrical conductivity proceeds mainly via reflection due to the skin effect [20, 21]. The electric field of a plane wave penetrating a conductor drops exponentially with its increasing depth (**Eq. 3**). In recent years, one can observe a strong tendency to resign from materials exhibiting high reflection losses, mainly because reflected radiation interferes with the surrounding electronic devices. And therefore, materials of higher absorption and lower reflection are preferred [22].

As a consequence of the above conclusions, typically in the *stealth* technology, composites exhibiting appreciable electrical conductivity and high SE_A are used. Nevertheless, the attenuation of EM-waves via absorption (which is dominant for CNTs) produces heat in the shielding material operating via absorption. The heat can be swiftly dissipated only if the shield is a good thermal conductor such as CNT [18]. The conductivity requirement for a 'good' EMI shielding composite is ~10^{-4} S/cm or higher. Higher electrical conductivity gives greater amount of nomadic charges which leads to more pronounced reflectivity [23]. Moreover, at low frequencies the attenuation proceeds almost exclusively by reflection (absorption can be neglected) and the whole shielding process becomes frequency independent. In the case of higher frequencies, the attenuation is of a dual character (reflection and absorption compete), but now penetration becomes the critical aspect (SE_R decreases with the increase in frequency) and at higher frequencies highly absorptive material should be used.

4. Radar absorbing materials

RAMs serve as radar shields and obviously the primary shielding mechanism of shielding here is absorption. The aim is to reduce Return Loss (*RL*) expressed by **Eq. 11** [24]:

$$RL = 10\log\left(\frac{P_{\text{in}}}{P_{\text{ref}}}\right) \quad \textbf{(Eq. 11)}$$

where:

P_{in} – the intensity of the incident radiation, W sr^{-1}

P_{ref} – the intensity of the reflected radiation, W sr^{-1}

In order to eliminate the reflected radiation, one must consider two possibilities. First, let us consider conditions when the reflectance (*R*) equals zero. For this purpose, let us use **Eq. 12** [25,26]:

$$R = \frac{P_{\text{ref}}}{P_{\text{in}}} = \text{Re}\,\frac{\underline{Z} - \underline{Z}_0}{\underline{Z} + \underline{Z}_0} \quad \textbf{(Eq. 12)}$$

where:

$\underline{Z}$ – impedance of the object, Ω

$\underline{Z}_0$ – impedance of the medium, Ω

Reflectance is zero when the numerator is zero, and thus the impedances of the object and the medium are equal. Impedance ($\underline{Z}$) defines the relationship between electric and magnetic field (**Eq. 13**) [27]:

$$\underline{Z} = \frac{\underline{E}}{\underline{H}} = \sqrt{\frac{\underline{\mu}}{\underline{\varepsilon}}} \quad \textbf{(Eq. 13)}$$

where:

$\underline{E}$ – component of the electric field intensity vector in **r** direction, V m^{-1} (N C^{-1})

$\underline{H}$ – component of magnetic field strength vector in **r** direction, A m^{-1}

$\underline{\mu}$ – complex form of the permeability, H m^{-1}

$\underline{\varepsilon}$ – complex form of the permittivity, F m^{-1}

Permittivity (ε) is represented as a sum of the real (ε') and imaginary (ε'') component (**Eq. 14**), similarly to permeability ($\underline{\mu}$) (**Eq. 15**):

$$\underline{\varepsilon} = \varepsilon' + \text{i}\varepsilon'' \quad \textbf{(Eq. 14)}$$

$$\underline{\mu} = \mu' + i\mu'' \qquad \textbf{(Eq. 15)}$$

The real component is a measure of energy stored in the object, while the imaginary one is a measure of dispersed energy. The circular motion of dipoles leads to changes in the value of both components at the frequency of relaxation. At frequencies below this value, lowering the value of the imaginary component is proportional to the frequency of radiation. Conversely, when the frequency increases, ε'' also increases, while, simultaneously, ε' decreases. This behaviour takes place because the dipoles have no time to align according to the lines of external field. When frequency is higher than frequency of relaxation, both components are declining because the field is changing too rapidly to become polarized [28]. When the material is composed of more than one component, the charge carriers cannot migrate at the same speed throughout its whole volume. This non-uniformity leads to their localization and accumulation at the interfaces. The accumulation interferes with the electric field and increases both capacitance and the real component of electrical permittivity of the whole material [9].

One might also eliminate the reflection using materials capable of absorbing radiation. According to the Beer's Law, the absorbance is proportional to the thickness of the absorbing layer. From the economic point of view, it is preferred however when thickness of the absorbing layer is reasonably small. In this case, in order to ensure maximum of absorption, material of the highest permittivity and permeability should be used [29].

For radar shielding applications rarely a single material can meet the technical constraints, and so, composites are the preferred ones. Such composites consist of conductive filler and the insulating polymer matrix. The composites become electrically conductive beyond a critical concentration of the conducting filler called *percolation threshold* (**Eq. 16**) [30,31]:

$$\sigma_C = A(V - V_C)^X \qquad \text{(Eq. 16)}$$

where:

σ_C – conductivity of the composite, S m^{-1}

V – volume fraction of the filler, dimensionless

V_c – volume fraction of filler corresponding to the percolation threshold, dimensionless

A – conductivity of filler, S m^{-1}

X – constant (critical exponent), dimensionless

Percolation threshold can be reduced by using one-dimensional (1D) nano-size conductive fillers. The higher aspect ratio of the filler, the lower is its concentration needed for achieving the percolation threshold [32].

5. Properties of CNTs – implications for the *stealth* technology

CNTs as quasi one-dimensional sp^2-allotrope of carbon were 're-discovered' in 1991 by Sumio Iijima [33,34]. Although the individual CNT exhibits excellent electrical, thermal and mechanical properties, CNTs in bulk form black powder indispersible in all non-reactive solvents. This insolubility reflects high molecular weight, abundant van der Waals forces between individual CNTs, (super)hydrophobicity and large surface area [35,36]. Hence, pristine (or as-synthesized or non-functionalized) CNTs tend to aggregate and their processing is troublesome. The appropriate surface modification and choice of solvent, dispersing agent and/or polymer matrix might allow for achievement of fine and stable CNT dispersions. Reaching the sufficient dispersibility is crucial to obtain effective MW-absorbers [37,38]. Moreover, from the point-of-view of *stealth* technology and manufacture of RAMs, there are few properties of matrix-dispersible CNTs which also play an important role [39,40]: RAMs should be lightweight, chemically resistant, of high mechanical performance, conveniently processable and inexpensive.

Electron transport in CNTs may show ballistic character, i.e. without scattering. Electrons can travel along the axial directions over the micrometer-range distances, but when a length of the CNT increases diffusive transport cannot be neglected. Moreover, dominating ballistic transport is suppressed at higher temperatures due to decreased mean free path of electrons as a consequence of increased scattering. Furthermore, because electron transport proceeds on the CNT surface, it can be affected by: (a) graphene lattice disorders (vacancies, substitutions, pentagon-heptagon defects), (b) intended (doping) or non-intended (contamination) modifications (e.g. residual aromatic hydrocarbons or amorphous carbon, processing residues, adsorbed molecules from atmosphere), and (c) physical distortions (strains, twists). Disorder centres lead to additional scattering and increasing resistance. The most common are Stone-Wales defects – four hexagons are replaced by a pair of 5- or 7-membered rings [41]. Selective growth of high-purity SWCNTs at industrial scale is still difficult and most of the synthetic protocols produce mixtures of CNTs with random *n*- and *m*-values [42]. One of the strategies to obtain material of desired properties is to control the CNT diameter or length, which indirectly affect electrical properties in terms of extension of conductive pathway and

elimination of less favourable chiralities. Such an approach is nevertheless unproblematic today as it depends on temperature, pressure, catalyst particle size and composition as well as carbon source [43]. In general, for a given CNT network and volume fraction in the isotropic composite, the overall electrical conductivity increases with an increase in the CNT length or a decrease in the CNT diameter [44,45].

Magnetic properties of RAMs based on intrinsically diamagnetic CNTs are governed by ferromagnetic or superparamagnetic catalyst particles encapsulated in the CNTs after synthesis – this approach constitutes endohedral functionalization and is achievable *in situ* during the nanotube growth. Magnetic properties of endohedrally functionalized CNTs derive from nanotube and metal characteristics as well as distribution, loading and metal nanoparticle dimensionalities. Exohedral functionalization with magnetic nanoparticles is obviously also possible via sol-gel techniques, electroless deposition, sputtering etc.

Since RAMs dissipate energy as heat and the infrared signature needs to be reduced, thermal properties of CNTs play an important role in the *stealth* technology. Obviously, the infrared signature is a fingerprint in detection of the object; hence, materials combining both electrical and thermal high-performance are greatly desirable. CNTs conduct heat via two mechanisms: electron-phonon interactions (depending on the structures of electronic bands and electron scattering) and phonon-phonon interactions (depending on the lattice vibrational modes) [46]. For semiconductors, at room temperature, phonon-phonon interactions play a main role, whereas electron-phonon interactions are negligible due to the large band gap and low density of free electrons. The phonon mean free-path in the axial direction for CNTs is much longer than for other materials. Consequently, thermal transport in CNTs is of a ballistic nature. Thermal conductivity of CNTs is a function of their length, diameter and chirality. Their high thermal conductivity derives from strong and rigid C-C bonds able to efficiently transport energy. SWCNTs and MWCNTs have high thermal conductivity along the axis, while in the radial direction, it is much lower due to non-covalent character of the interlayer bonding [47,48].

Both synthesis and modification step are crucial in terms of CNTs properties. Using CNTs as RAMs and EMI shields requires synthesis of CNTs with the appropriate length, diameter, chirality – essentially free of impurities and defects. All of these parameters affect mechanical, thermal and electromagnetic properties. Some properties may be improved in the additional modification steps (i.e. introduction of metal nanoparticles may improve electrical

properties due to decreased junction resistance between individual CNTs). However, we need to bear in mind that most of modifications are commonly destructive and may impair the shielding performance. Lastly, one should not forget about light-weight and carbon biocompatibility which are also important parameters. Importantly, current commercial price of industrial grade CNTs is as low as 50 $/kg (comparable to carbon fiber). Those market facts influence broader scope and larger scaling-up of the materials based on CNTs [49].

6. CNT composites/hybrid materials as RAMs and EMI shielding materials in comparison with accessible scientific data and commercial / patented solutions

Metals, due to high electrical conductivity, are the most commonly used shielding materials. However, high density, susceptibility to corrosion and the fact that metals are easily exposed due to reflection of the metallic gloss [50,51] has motivated a pursuit for alternatives. Conductive polymers (CPs), with 'programmable' mechanical properties (e.g. flexibility or rigidity), low density and inexpensive costs of a large-scale production, have been applied as the next generation EMI shielding materials. However, what has always been an impediment was their electrical conductivity, which is still much lower than that of metals. That is why, in the EMI shielding composites, polymers are commonly used as insulators, while conductivity is provided by the second component, typically metal micro- and nanoparticles (NPs) [52].

CNTs have recently emerged as an interesting alternative to metals. They are excellent electrical and heat conductors as well as 1D-fillers capable of forming conductive networks due to high aspect ratio. The conductive networks allow for propagation of the electrons, and thus overcoming high resistance of the insulating matrix. EMI shielding ability of CNTs increases with their increasing conductivity. This relationship arises from the proportional relationship between the absorption coefficient and electrical conductivity [53,54].

In general, carbon-polymer composites can be applied to absorb electromagnetic radiation at MW and radio frequencies. Absorption in the MW-range can be also associated with polarization of the RAM dipoles. The electric field interacting with a dipole generates its torque. The dipole is polarized orienting itself according to the direction and sense of the electric field. The rate of dipole re-orientation depends on the intensity and frequency of the electric dipole radiation. When the frequency is low, the dipole has a sufficient amount of time to align in accordance with lines of the field. In turn, when the frequency is higher, a delay in the alignment occurs associated with viscosity of the material. These are the

movements of dipoles causing internal friction and leading to dissipation of energy as heat [48].

Since typically resistance of CNT assemblies is higher than for metals, their larger volume fraction is required to reach the same performance. Conductivity of the composite can also be increased by introduction of metallic elements (e.g. Au, Fe, Co or their alloys) into the inner cavity of CNTs and between the individual CNTs in order to alleviate the junction resistance. Since hybrid materials can be designed to respond to both components of the electromagnetic wave, suppression of ths electric component can be provided by CNTs themselves whereas attenuation of magnetic component might be obtained by ferromagnetic additives, e.g. Ni, Fe or Co nanoparticles [24]. Here, CNTs come to the action as the most promising nanofiller. However, due to extensive agglomeration, CNT incorporation into the polymer matrix might require surface functionalization as a preliminary treatment [55].

In order to determine *SE* – from the analytical point of view – determination of magnetic and electrical characteristics in the frequency domain is required. As shown earlier, reflection or absorption of electromagnetic radiation depends on permittivity, permeability and conductivity of the material. In the frequency domain, the typical measurement technique is examination of the network element using vector network analyzer (VNA). VNA is a two-port instrument measuring the frequency spectrum of scattering parameters. In the basic electric and magnetic characterization of a given material, its spatial arrangement in the coaxial cable (as internal conductor or external insulator) can be applied. The results presented below with the measured *RL* and *SE* represent hence the data set allowing for design of the optimal shields.

The most challenging issue is to translate very promising *SE* values observed for the unmodified (pristine or ‘as-synthesized’) CNTs into the macro-scale. With still only a few examples of scalability of CNT macro-assemblies production, one must admit that large-scale manufacture of CNT-based effective EMI shielding materials must currently involve physicochemical modification of CNTs. The character of those modifications is crucial to preserve or enhance their electromagnetic properties as compared to pure CNTs. For instance, it is known that CNTs as 1D π-conductors can be excellent EMI shielding material, but the outer CNT layer might have a significantly lower conductivity due to high dissipation of electricity at the points of contact. The key issue becomes hence the adequate dispersion of CNTs in the matrix allowing for the formation of electrically conductive network, i.e. above

the percolation threshold [56]. On the other hand, CNTs may display magnetic properties as a result of the presence of encapsulated residual catalyst NPs from the synthesis. Iron-based NPs provide a stronger magnetic saturation with lower coercion and consequently, higher magnetic permeability [57]. *SE* of CNTs composites at various radar ranges are presented in **Table 1**. In order to enable a direct comparison between different CNT-based materials, *SE*-values were normalized to thickness of the composite/hybrid and type as well as the values of nanofiller content were included [31,58-86]. However, it must be emphasized that in none of the CNT-based composites and hybrid materials from **Table 1** mechanism of shielding was not identified, e.g. by VNA technique.

Table 1 *SE* for CNT-based composites and hybrid materials elaborated in scientific publications

Radar range	Matrix	CNTs type	Additive	CNT *OD/l* [nm/μm]	CNT [wt.%]	*SE/t* [dB mm^{-1}]	Ref.
UHF L S	CNCR	MWCNTs	-	9.5/1.5	3	0.3	58
	ER	MWCNTs	Ni@	10-25/n.d.	1	7	59
		MWCNTs	-	2-15/1-10	0.1	10-7.5	60
		F-MWCNTs	-	2-15/1-10	0.1	15-12.5	
	PMMA	MWCNTs	-	10-50/1-25	4.76	15-20	61
		MWCNTs	Co@	n.d./ n.d.	20	45	62
		MWCNTs	Fe@	n.d./ n.d.	40	67.5	
	PE	MWCNTs	-	10/10-20	18	16.7-20	63
	MF	MWCNTs	-	5/1-2.5	50	35	64
	LCPs	MWCNTs	-	5/1-2.5	50	40	
		MWCNTs	-	10/100	50	55-60	
X	ER	SWCNTs	-	5.32/0.74	3	5	65
		SWCNTs	-	5.95/1.43	3	6	
		O-MWCNTs	MnZn	10/1-5	4	8.5	66
		O-MWCNTs	15% Fe	50/10-20	15	20-23.3	67
		O-MWCNTs	15% Fe_3O_4	50/10-20	15	20-23.3	
	PU	MWCNTs	-	50/10-20	4.8	7	68
		O-MWCNTs	-	10-70/300	10	19.3	69
		MWCNTs	Cu-Ni	20-30/10-30		26.7-33.3	56
		MWCNTs	-	50/10-20	76,2	100	68
		SWCNTs	-	5.95/1.43	20	178.5	70
		MWCNTs	-	10-50/1-10	25	240	71
	IIR	SWCNTs	-	25/<10	8	9	72
	SN	MWCNTs	10% @Co	10/n.d.	2,7	10	73
	PMMA	Mah-g-MWCNTs	-	10-50/1-25	4.76	9-18	74
		MWCNTs	-	10-50/1-25	4.76	20-30	61
		Br-MWCNTs	-	10/1.5	7.3	42.1	31
		MWCNTs	@Co	n.d./ n.d.	20	45	62
		MWCNTs	@Fe	n.d./ n.d.	40	67.5	
	PPC	MWCNTs	-	2.8/35-50	15	14	75
		MWCNTs	-	9.5/1.5	15	20	
	CNTR	MWCNTs	-	60/15	15	14	76
	PAN	O-MWCNTs	-	5-10/5-10	10	16.7	77
	PS	MWCNTs	-	10/10	20	25-30	75
	PDMS	MWCNTs	-	10-20/50-200	5,7	36-40	78
	PE	MWCNTs	-	9.5/1.5	10	50	79
K_u	IIR	SWCNTs	-	25/<10	8	5-6.8	72
	S.C.	MWCNTs	-	60-100/2-5	8	13.3-18	80
	ER	O-MWCNTs	15 % Fe	50/10-20	15	13.3-20	67
		O-MWCNTs	15% Fe_3O_4	50/10-20	15	13.3-20	
	PMMA	Mah-g-MWCNTs	-	10-50/1-25	4.76	15-18	74
		MWCNTs	-	10-50/1-25	4.76	20-25	61
		Br-MWCNTs	-	10/1.5	7.3	26.3-31.6	31
	PEDOT	MWCNTs	-	20-50/50-100	15	16.1-21.4	79
	PTT	MWCNTs	-	10/20-30	10	18.8-21.3	81
	PANI	MWCNTs	-	10/<10	25	40	82
	PP	MWCNTs	-	10-12/20-30	10	25	83
K K_a	ER	O-MWCNTs	15 % Fe	50/10-20	15	6.7-13.3	67
		O-MWCNTs	15% Fe_3O_4	50/10-20	15	6.7-13.3	
	SMP	MWCNTs	-	150/10-20	6.7	10-13.3	84
	FS	MWCNTs	-	20-40/5-15	10	11-14	85
	PMMA	Br-MWCNTs	-	10/1.5	7.3	35.1-52.6	31

CNCR – concrete, ER – epoxy rubber, F – fluorinated, O – oxidized, MF – melamine formaldehydes, LCPs – liquid crystal polymers, IIR – butyl rubber, Mah-g – maleic anhydride grafted, Br – brominated, SN – silicon nitride, ceramics, PPC – polypropylene random copolymer, CNTR – cement, SC – silica composites , PTT – poly(trimethylene terephthalate), SMP – shape memory polymer, FS – fused silica, n.d. – no data

For the UHF/L/S range, the highest normalized *SE*-values (SE_N) were achieved for the Fe@MWCNTs-PMMA composite. This high value corresponds with as high as 40 wt.% MWCNTs content. Interestingly, substitution of MWCNT-encapsulated iron NPs by cobalt NPs resulted in slightly lower SE_N, though the MWCNTs content was also lower (20 wt.%). It is worth mentioning that for F-MWCNTs-ER composite (based on fluorinated MWCNTs) SE_N equalled 15 dB only for 0.1 wt.% MWCNTs. Higher SE_N value could be related to catalyst particles impurities in CNTs (CNTs in LCPs matrix) or better dispersion in matrix (higher SE_N for LCPs composite than for MF composite) [60, 64].

For the X-range, the highest SE_N were achieved for the MWCNT-PU composite. For 25 wt.% of the MWCNT content SE_N was as sky-rocketing as 240 dB mm^{-1}. Relatively high values were also achieved for Fe@MWCNT-PMMA composite, but at the much higher MWCNTs content. Similarly, high SE_N-values, but for low MCWNT content, were achieved for MWCNT-PDMS and MWCNT-PE composites. One must here recall again the importance of CNT dispersion in polymer matrices. For the same content (10%), SE_N is higher for PU composite than for PAN composite. It is related to a much better quality of dispersion in the PU-matrix associated with a formation of hydrogen bonding between carboxylic groups in CNTs and PU-chains (in urethane –NHC(=O)O moieties). Those interactions result in the enhancement of electrical conductivity of the composites and consequently better shielding performance [62, 71, 78, 79].

For the K_u-range, the highest SE_N were achieved for MWCNT-PANI composites with 25 wt.% MWCNTs content. A rather high SE_N was attained for Br-MWCNT-PMMA composite (with brominated MWCNT-filler) which provided high SE_N-values also in the other K-ranges (K, K_a). For this composite, the MWCNT content was only 7.3 wt.% [31, 82]. The obtained data confirm theory that in lower frequency ranges, reflectivity is the dominating mechanism, whereas in higher the mechanism is based on absorption. For the same sample (with Fe) SE_N is higher than 20 dB mm^{-1} (X-range), 13,3 dB mm^{-1} (K_u-range), while for K- and K_a-ranges SE_N value is lower (<13.3 dB mm). In lower frequency, the reflection losses associated with Fe NPs play an important role in shielding, hence SE_N value is higher. This relationship is not observed for samples with encapsulated metal particles for which SE_N value is frequency-independent (Fe@MWCNTs in PMMA matrix).

The electric and magnetic properties of CNTs can be enhanced by their amalgamation with metallic elements, particularly with metallic NPs. Those elements (‘additives’) might improve

electrical conductivity of CNTs and their magnetic response [40]. As mentioned above, pristine CNTs are not effective RAMs because of too low magnetic losses. On the other hand, metallic magnetic NPs used separately are susceptible to oxidation. As the optimized solution, encapsulation of metallic NPs in CNTs provides a protective layer against oxidation and excludes their tendency to agglomeration. It was pointed out that the encapsulation of iron into MWCNTs (outer diameter 20-40 nm, length 5-15 μm), at a 1 mm-thick layer of Fe@MWCNT-epoxy composite, increased *RL* up to 33 dB (**Fig. 5**) [86]. Modification of MWCNTs by Fe NPs led then to absorption of as much as 99.9% of the incident radiation. Fe@MWCNTs were also dispersed in other polymer matrices. It turned out that density of the Fe@MWCNT-epoxy resin composite was twice as high as compared to the pure MWCNT-based one. Although the Fe-MWCNT composite contained many defects such as vacancies, kinks or suspending bonds, they were found as responsible for multiple reflections and internal polarization of the wave. This phenomenon allowed for the more efficient shielding via absorption. As authors claimed, the encapsulation of iron might produce Stark effect, i.e. of splitting of electron energy levels by the action of electric field. Thus, Fe-modification of the composite has increased the number of available energy levels allowing for the more efficient absorption [87,88].

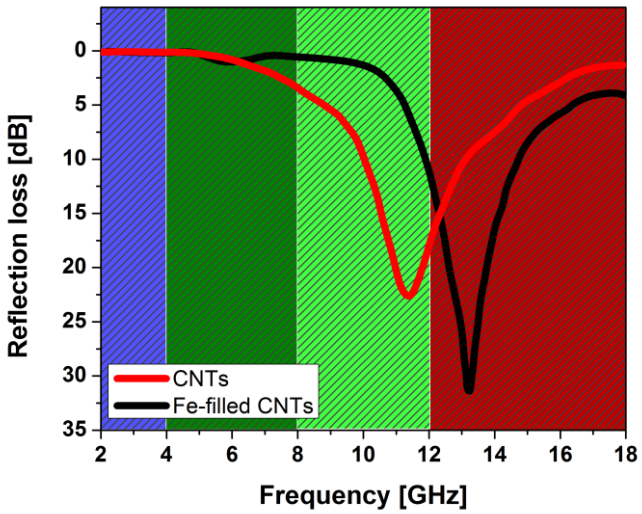

Fig. 5 Reflection losses of CNTs and Fe@CNT-epoxy resin as function of frequency; modified and reproduced with permission from [86]. Copyright Elsevier, 2015

Improvement of electrical and magnetic properties in the CNT-based composites can be achieved not only by using Fe NPs, but also other ferromagnetic NPs. For instance, Lin et al. filled MWCNTs (inner diameter between 60-80 nm and length up to several micrometers) with Co NPs. For the studies of MW-absorbing properties, Co@MWCNTs were mixed with

paraffin (20 wt.%) [89]. *RL* of modified MWCNTs was higher (15 dB as compared to 5 dB for the unmodified MWCNTs) at the same frequency. Moreover, with the increase in the composite thickness, the maximum of *RL* exhibited bathochromic shift (**Fig. 6**) and simultaneously, the absorption range has expanded.

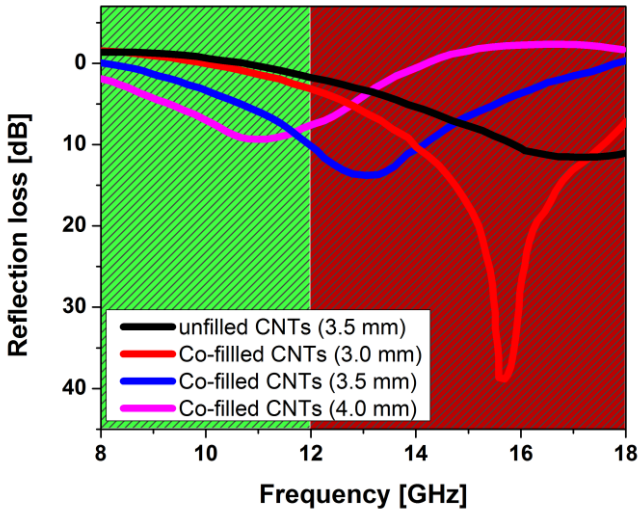

Fig. 6 Reflection losses of MWCNTs and Co@MWCNTs depending on frequency and thickness of the composite modified and reproduced with permission from [89]. Copyright Elsevier, 2015

A very promising solution was modification of MWCNTs with Cu-Ni NPs. Due to high electrical conductivity, they were found as generating higher induction currents which, in the same time, suppressed penetration of the material. In the same time, Cu-Ni nanofoams had lower density and yielded losses due to multiple reflection and scattering (**Fig. 7**). The effect of introduction of MWCNTs (outer diameter 20-30 nm, length 10-30 μm) was studied in PU-matrix of 1.5 mm thickness. In the case of pure Cu NPs of high electrical conductivity, the shielding mechanism was mainly related to absorption losses and scattering. For Ni NPs, the mechanism was based mainly on absorption losses. Additionally, the porous composite structure enabled for multiple internal reflections, making difficult to escape the radiation from its interior prior to absorption and conversion to heat. This composite, depending on the thickness, achieved *SE* of 54.6 dB which was much higher than the values obtained for the non-porous composite [56].

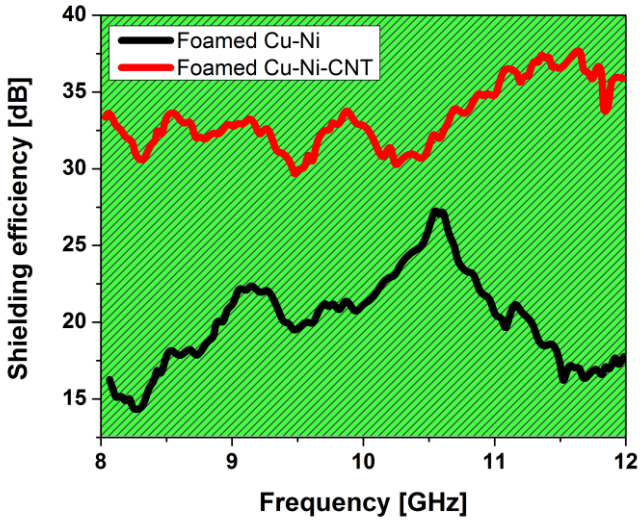

Fig. 7 Shielding efficiency of foamed Cu-Ni and Cu-Ni-MWCNTs in PU-matrix at different frequencies; modified and reproduced with permission from [56]. Copyright Elsevier, 2015

The aim of other studies was to reveal the impact of MWCNT-anchored metallic NPs on dispersion of MWCNTs in the polymer matrix. The most promising results have been obtained for Ni NPs. For a given concentration of Ni NPs, dispersion of MWCNTs was significantly improved (due to presence of nickel-based active group on the MWCNT surface) and considerably better electrical properties and hence higher *SE* [90] were achieved. This modification also allowed reducing contact losses between the individual MWCNTs by formation of more stable metal-metal junctions and strengthening the MWCNT-based electrical network [59].

Zhao et al. modified MWCNTs (outer diameter 10-30 nm; length 5-15 μm) by encapsulation of Ag nanowires as the most conductive metallic NPs [91]. In those studies, a 1 mm-thick epoxy composite was used. The shielding mechanism was found here as based primarily on dielectric losses. The introduction of Ag into MWCNTs resulted in the increase in both number of centres of multiple scattering and the interfacial polarization (charge imbalance as the effect of accumulation of charge at an interface between two regions of materials in the external field). With the increase in the Ag content in the composite, the absorption maximum shifted to longer waves range, wherein the unmodified MWCNTs had small *RL* (**Fig. 8**). The introduction of Ag into the MWCNTs did not improve shielding properties of the composite, but allowed for the extension of the shielding range [92].

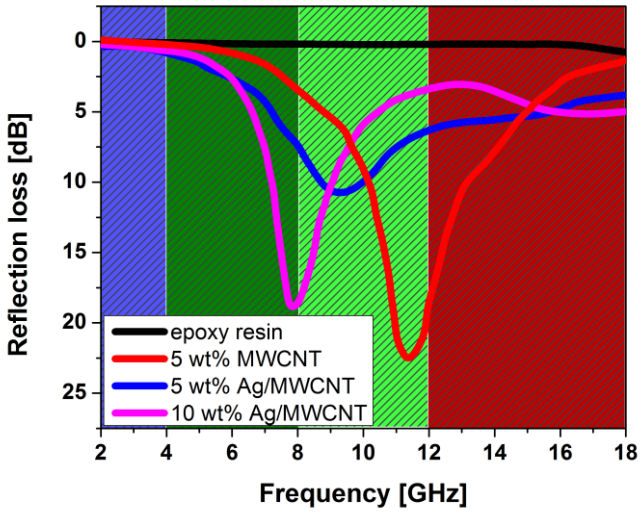

Fig. 8 Reflection losses of MWCNTs and Ag@MWCNTs versus epoxy resin; modified and reproduced with permission from [92]. Copyright Elsevier, 2015

Apart from metallic NPs, metal oxide NPs were also used as components in MWCNT-composites. A very interesting and promising solution was found by modification of MWCNTs with ZnO NPs. ZnO is a semiconductor for which the band gap is 3.37 eV while the exciton binding energy 60 MeV. ZnO-MWCNT system allowed to combine excellent suppressing properties of the 0D-material with a strong absorption in the MW range associated with higher anisotropy along the axial direction of MWCNTs. Moreover, the system was characterized by a resonant absorption mechanism [93]. ZnO NPs were deposited on the MWCNT surface to form a heterogeneous contact area and to strengthen polarization of the surface. Moreover, consumption of amorphous carbon layer on the MWCNT surface and generation of oxygen vacancies in ZnO NPs during the synthesis step, effected in higher production of charge carriers in electromagnetic field. This phenomenon has intensified relaxation of polarization and increased the dielectric losses. In the case of this composite, one could modify the efficiency of screening towards temperature-responding material (*SE* should increase with the increase of temperature). In addition, under the influence of electromagnetic field, charge carriers from the oxygen vacancies have migrated which led to relaxation of polarization. For the composite with a low fraction of the filler, a typical increase in *SE* was observed, e.g. 70 dB for ZnO-MWCNT-glass composite with a 3 wt.% nanofiller loading. What is interesting, further increase in the content caused a decrease in *SE*. As authors explained, difference between impedance of the composite and the medium resulted in strong reflection [94].

Arjmand and Sundararaj [95] studied electromagnetic properties of nitrogen-doped (3.85 at. %) versus pristine MWCNTs, both embedded in PVDF matrix. It was found that doping changed the MWCNT structure into more rigid. The properties of N-doped MWCNTs were affected by a nature of C-N bonds. The pristine MWCNTs-based composite was characterized by improved dispersion, increased electrical conductivity, and a lower percolation threshold. *SE*, at the same content of MWCNTs, was sixteen times higher for the composite based on the undoped (pristine) MWCNTs (**Fig. 9**).

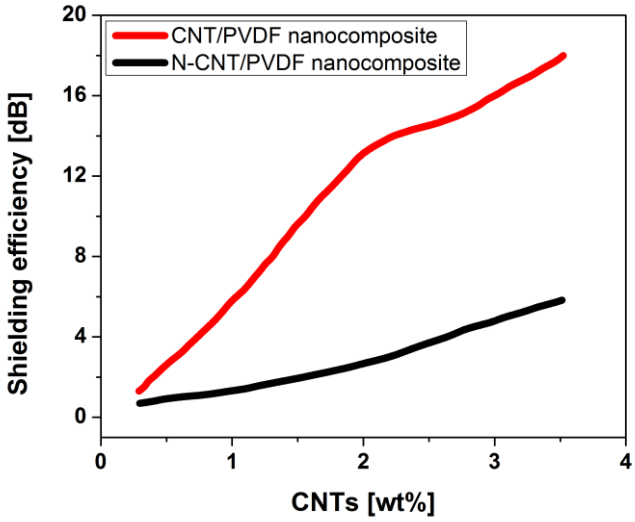

Fig. 9 Shielding efficiency of N-doped and undoped MWCNTs-PVDF nanocomposite; modified and reproduced with permission from [95]. Copyright Elsevier, 2015

N-MWCNTs had smaller length and larger diameter than the undoped counterparts, and consequently, lower aspect ratio which effected higher percolation threshold and lower electrical conductivity. Moreover, the morphology of N-MWCNTs strongly depended on type of the catalyst (bamboo-like for Fe, open-channel for Co and Ni).

As mentioned, a high content and homogenous dispersion of the MWCNT-filler in the composite could be achieved by functionalization. On the other hand, oxidative covalent modification of CNTs diminishes their aspect ratio, and thus electrical conductivity [96,97]. Zakharychev et al. [97] used nitrating mixture (sulfuric and nitric acid (3:1; *v/v*), 90 °C, 0.5-15 h) to oxidize MWCNTs. The functionalization was accompanied with degradation of external CNT walls and yielded increased hydrophilicity. The contribution of carboxyl groups depended on the functionalization time intervals (2 wt.% for 0.5 h; 4.3 wt.% for 15 h). After 15 h, O-MWCNTs were eight times shorter than unmodified MWCNTs. A synergic effect of physical (non-covalent modification by surfactant) and chemical modification emerged as a

route to lower percolation threshold observed for sterically and electrostatically stabilized O-MWCNT-network. Furthermore, π–π interactions are important filler-matrix connections as they affect the dispersion and percolation threshold. They also promote transfer of electrons from MWCNTs to the matrix thereby improving absorption of radiation. Hence, aromatic polymers were frequently studied as EMI shielding matrices, e.g. polystyrene (PS) [98] or epoxy resins [99]. Other CNT-based composites were based on PMMA [31], PU [24,100], PE [101] or PVC [102].

In order to eliminate oxidation, MWCNTs were increasingly used in the *in situ* polymerizations or *ex situ* dissolution of nanotubes in the polymer matrix [103, 104]. Improvement in the quality of dispersions could also be obtained by fluorination of nanotubes. This treatment also reduced contribution of amorphous carbon in the nanotube samples and led to higher *SE*-values [17 dB versus 28 dB for unmodified MWCNTs and F-MWCNTs (5.4 at.% F), respectively] [60].

Another factor playing a significant role in 'programming' of electromagnetic properties of CNT assemblies is the CNT orientation in the composite with a respect to the plane of polarization of incident radiation. This effect has been studied for the MWCNT-epoxy resin composites with nanotubes of parallel and perpendicular alignment to the incident radiation. For the 0°-angle, negative values of the real component of permeability were found. In addition, those values were very frequency-sensitive. On the other hand, for the 90°-angle, the real component of permeability was positive and only slightly fluctuated. A different situation was observed for electrical conductivity. Electrical conductivity measured in the parallel direction (in agreement with the nanotube alignment direction) was five times higher than for the perpendicular direction. The high electrical conductivity correlated with a large *SE*. Additionally, *SE* was significantly higher in a multi-layer CNT system for a sandwich-type arrangement (15 dB for monolayer as compared with 68 dB for a five-layer system which corresponds to the linear relationship) [105].

Verma et al. studied the influence of nanotube aspect ratio on the electromagnetic properties of MWCNT-polypropylene carbonate (PPC) composites. A higher packing density and better dispersion were achieved for shorter MWCNTs (aspect ratio of 160). Also, shorter MWCNTs had higher surface area have been translated into better wettability and larger number of sites involved in the interaction with the matrix. This is particularly advantageous from the mechanical properties point of view. On the other hand, for longer MWCNTs (aspect ratio of

1400-2000), a better charge transport and lower percolation threshold were obtained. Here, 10 times higher electrical conductivity (at the same MWCNT content in the matrix) was achieved. The introduction of MWCNTs into polymer has dramatically increased *SE* (0.3 dB for PPC, 8 dB for as low as 0.5 wt.% of MWCNTs). Further, the presence of MWCNTs contributed in the increase of *SE* to 10.8 dB (4 wt.%) and 37.8 dB (15 wt.%) for short and 16.2 dB (4 wt.%) and 26.9 dB (15 wt.%) for long MWCNTs, respectively. The obtained results mean that longer MWCNTs have superior shielding properties at lower loadings, but with a greater MWCNT content, the superior shielding properties were obtained for shorter MWCNTs. This behaviour must have been related to the dominance of a particular shielding mechanism depending on the MWCNT content in the matrix (**Fig. 10**). And so, with a lower MWCNT content, much better MWCNT dispersions were achievable and the *SE* primarily depended on the aspect ratio. When MWCNT content was higher and MWCNTs tended to agglomerate, higher *SE* was achieved for shorter MWCNTs due to homogeneous dispersion. Importantly, both short and long MWCNTs had constant *SE* in the X-band [75].

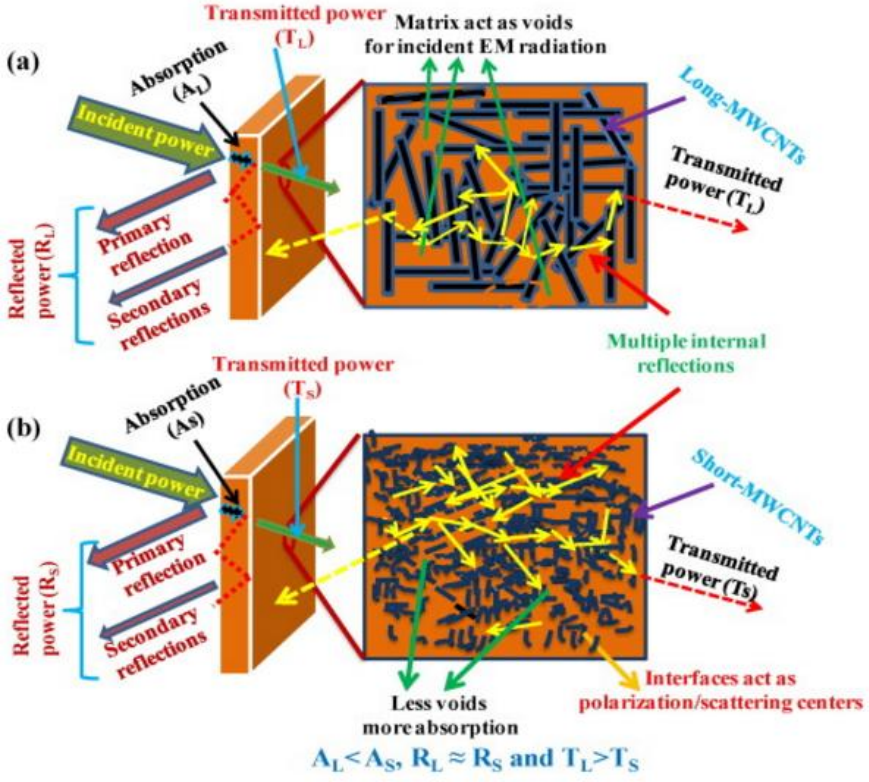

Fig. 10 EMI shielding mechanism of the MWCNTs-PPC composite; reproduced with permission from [75]. Copyright Elsevier, 2017

The properties of CNT composites were affected by their processing technology. Arjmand et al. revealed differences in the properties of MWCNT-PS composites processed by two different techniques. The first differences were related to morphology of the composite. The composite produced by injection moulding had a uniform MWCNTs dispersion without significant agglomeration. In the case of compression moulded composite, MWCNTs were inhomogeneously distributed in the polymer matrix. This technique also affected electrical conductivity: the composite obtained by injection moulding had lower electrical conductivity (higher percolation threshold). This fact is derived from the uniform alignment of MWCNTs in the matrix resulting a decrease in the number of junctions between individual CNTs. *SE* of the composites equalled to 25.4 dB (5 wt.%) and 63.6 dB (20 wt.%) versus 15 dB (5 wt.%) and 30 dB (20 wt.%) for the compression and injection moulded composites, respectively (**Fig. 11**). Both composites exhibited similar *SE* throughout the whole X-band. In addition, it was verified whether processing technique affected the shielding mechanism. As mentioned earlier, reflective mechanism requires mobile charge carriers such as electrons or holes which interact with the incident radiation. In both cases, as expected, it was observed that increased efficiency of reflection was correlated with the increasing content of MWCNTs in the matrix. The relationship between electric conductivity and the reflectance mechanism explains higher *SE*-values for the compression moulded technique. Comparable *SE*-values could be associated with a comparable surface area of MWCNTs interacting with radiation – regardless of their arrangement in the matrix. *SE* via absorption increased with the increasing MWCNT content (increase in the number of charge carriers, real and imaginary components of permeability) and decreased with the increasing arrangement [106].

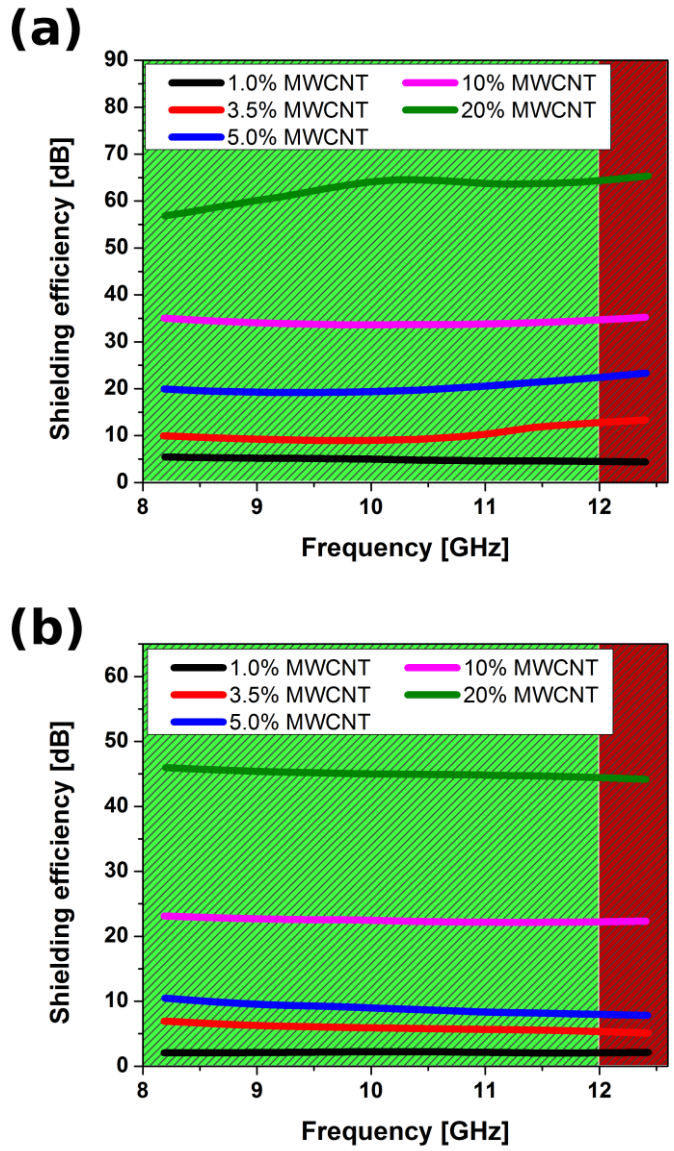

Fig. 11 Shielding efficiency of MWCNT-PS composites of various CNT content as a function of frequency for (**a**) compression moulded and (**b**) injection moulded samples; modified and reproduced with permission from [106]. Copyright Elsevier, 2015

A MWCNT-PMMA foam composite exhibited a better reflected to absorbed radiation ratio while *SE* in total has increased with the decreasing size of pores. The composite structure provided a dense conductive MWCNT-network of a high permittivity. A different mechanism for the layered MWCNTs composite was observed. In this case, multiple reflections between the layers were found as a dominant phenomenon. Multiple reflections have lengthened the path radiation must have overcome within the composite – hence its absorption capacity increased [31].

One of the most promising strategies to make EMI shielding materials is combining CNTs with CPs. The so-formed composites have typically high *SE*-values. The vast majority of the

previous studies were related to CNT-polyaniline (PANI) composites since PANI is one of the most versatile CP. It has low density, considerable thermal and chemical stability as well as high conductivity in a broad range of MW-frequencies. Moreover, it shows substantial affinity to the CNT surface [103,104,107]. And so, a simple coverage of O-MWCNTs with PANI increased permittivity, permeability, dielectric loss, diamagnetic loss and *SE* (**Fig. 12**) [50]. Moreover, *SE* increased not only with the increasing O-MWCNT content but also with the PANI content. Furthermore, PANI considerably affected the frequency for which the maximum *RL* was produced. Thicker PANI layers led to stronger absorption and the absorption maximum was shifted toward lower frequencies [108,109]. It must be noted that the conductivity of PANI was also affected by conditions of its synthesis, such as temperature, a monomer/oxidant ratio and time of polymerization. The main interactions between O-MWCNTs and PANI were indicated as π-π bonding and hydrogen bonds between the carboxyl groups of oxidized MWCNTs and amino groups of the monomer. Intensity of those interactions has escalated with the increasing adsorption of aniline on the O-MWCNT surface and has led to higher electrical conductivity of the *in situ* produced composite. In addition, the O-MWCNTs served as conductive bridges connecting PANI domains thereby improving electrical conductivity [110].

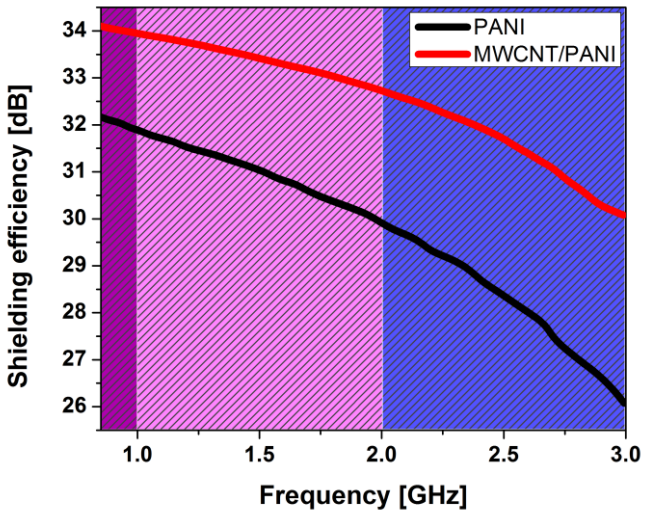

Fig. 12 Shielding efficiency of PANI and MWCNTs-PANI composite modified and reproduced with permission from [50]; copyright Korean Carbon Society, 2011

For comparative purposes, commercial solutions for EMI shielding were collected in **Table 2**. They mainly exploit paints, but tapes, aerosols and wires insulation also have been reported. But importantly, all the forms of final preparations were characterized at low EM-frequencies.

Table 2 Commercially available EMI shielding materials

Trade name	Composition	Form	*SE* [dB]	Range
HSF 44	dispersing agent, graphite, water, CB, cellulose, surfactant, defoamer, preservative	paint	38	30 kHz – 300 kHz; 3 – 30 MHz
HSF 54	pure acrylate, graphite, water, CB, defoamer, dispersing agent, surfactant, cellulose, preservative	paint	37	30 kHz – 300 kHz; 3 – 30 MHz
HSF 64	potassium silicate, graphite, water, pure acrylate, CB, defoamer, dispersing agent, surfactant, cellulose, preservative	paint	39	30 kHz – 300 kHz; 3 – 30 MHz
HSF 74	potassium silicate, graphite, water, CB, defoamer, dispersing agent, surfactant, cellulose	paint	39	30 kHz – 300 kHz; 3 – 30 MHz
NSF 34	water, pure acrylate, CB, defoamer, dispersing agent, surfactant, cellulose, preservative	paint	40	30 kHz – 300 kHz
CuPro-Cote Paint	Cu microparticles (33-38 μm), aqueous base	paint	>75	1 MHz – 1 GHz
Ni/Cu/Co Fabric Shielding tape	Ni, Cu, polyester	tape	>64	30 MHz – 1 GHz
Air Pure Paint	water, acrylic dispersion, vinyl acetate dispersions, thickeners (cellulosic, polymeric), dispersing aids, Ni (26.4 wt.%)	paint	20	3 – 30 Hz
838 Total Ground Carbon Conductive Coating	CB (9%), acrylic resin, acetone, ethanol, toluene	paint	>50	<1 MHz
839 Super Shield Graphite Conductive Coating	graphite (14 %), CB (1%), acrylic resin, acetone, ethanol, toluene	paint	>50	<1 MHz
841 Super Shield Nickel Conductive Coating	Ni flakes (48%), acrylic resin, talc, toluene, acetone	paint	50±25	UHF L S C X K_u
842 Super Shield Silver Conductive Coating	Ag flakes (62%), acrylic resin, acetone, ethanol, toluene	paint	75±20	UHF L S C X K_u
843 Super Shield Silver Coated Copper Conductive Coating	Ag (5%), Cu (43%), acrylic resin, acetone, ethanol, toluene	paint	60±18	UHF L S C X K_u
Master Bond MB600S	Ag, water, sodium silicate, additives	paint	95-105 95-60 60	L S C X K_u
RFID67#L	Cu (23%), Ni (20%), polyester	fabric	70-84	30 MHz – 1.5 GHz
RFID67#r	Cu, Ni, polyester	fabric	74-92	30 MHz – 1.5 GHz
Ni Screening Compound Plus ERNSCP400H	dimethyl ether, butyl acetate, Ni (10-30%), ethyl acetate, propan-2-ol, methanol	aerosol	55-65	20 – 500 MHz
RS 568-483	Ni (25-50%), dimethyl ether, xylene mix, toluene, butyl ethanoate, propan-2-one, 2-methoxy-1-methylethyl acetate	aerosol	36-60	50 MHz – 1 GHz
Geovital T98	water, graphite, pure acrylic emulsion,	paint	<50	<10 GHz

Alpha	CB, additives, preservatives			
ECOS Interior EMR Shielding Paint	water, acrylic dispersion, thickeners, dispersing aids, Ni	paint	n.d.	30 Hz – 30 kHz

Most of the solutions were based on metallic layers, but an increasing number of carbon-related EMI shielding materials is emerging. It is important to note that the number of formulations based on metals is significantly higher than that of carbon, but the potential of CNTs has been only patented so far and it has not been nevertheless fully recognized by the market. And although few commercial solutions are – by declaration – available at this moment, a number of patents for CNT-based solutions is rather large and constantly growing (**Table 3**). Nonetheless again here, no division between reflection, absorption and multiple reflections was given.

Table 3 Summary of patented EMI shielding composites based on CNTs

Frequency range	Matrix	CNTs type	Additive	CNT *OD/l* [nm/µm]	CNT [wt.%]	*SE/t* [dB mm^{-1}]	Patent
n. d.	Thermoplastic resin	MWCNTs	Carbon fiber, metal NPs	9.5/1.5	1-8	14-21	US2014238736
L S	ionic liquid, polyamic acid, *N*-methyl-2-pyrrolidone, THF, toluene	MWCNTs	-	30-60/n.d.	>5	20-50	US2013005920
L S C X K_u	ABS copolymer	MWCNTs	Ni, carbon fibers	20-40/10-30	2	33-73	US2010311866
UHF C X K_u	solvent, surfactant, polymeric material	SWCNTs MWCNTa	Metal NPs, carbon nanofibers	1-5/n. d. 5-200/n.d.	4	10-15	US2008057265
n. d.	surfactant, solvent (methanol, ethanol, water), resins or polymers (formaldehyde or urea resins)	MWCNTs MWCNT-NH_2 MWCNT-COOH	-	n. d.	0.1-16	n. d.	NZ547245
S C X K_u	*N*,*N*-dimethylacetamide, methyl methacrylate, AIBN, PET	MWCNTs	-	10-50/1-25	0.5-10	10-55	TW200918586
X	natural rubber, cetyl trimethyl ammonium bromide, dicumyl peroxide	MWNCTs	-	9.5/1.5	0.5-5	10-45	CN105086012
X	polylactic acid	MWCNTs	-	9.5/5	0.2-1	3.7-13	CN105038160
UHF L S C X K_u	polymer matrix (polyester, polyphthalamide)	MWCNTs	Metal	8/1-10	1-20	40-130	JP2015144294
X K_u K K_A	polymer matrix (polystyrene, polycarbonate)	CNTs	graphite, metal particles (iron, nickel, cobalt)	n. d./n. d	0.5-3	30-60	KR20130125098
UHF	resin matrix, hollow glass microspheres, hardener, additives	MWCNTs	-	2-50/0.2-0.5	0.5-20	<40	US2011101284

Despite of small amounts of CNTs in shielding composites, they allow to achieve high *SE*-values in a broader range of frequencies as mentioned earlier. And among the modification steps, the introduction of ferromagnetic NPs dominates (enhancement of conductivity and magnetic properties). The second most popular CNT modification is an improvement of their compatibility with various matrices by polar functional groups. Those materials are used

mainly for EMI shielding of sensitive electronic devices, but many of them are used as conductive composites. The appropriate choice of the matrix-solvent pair allows to design various forms of composites, i.e. paints, films or membranes. One of advantages of CNT composites is independency of *SE*-values in certain frequency ranges. This property enables using those composites in a whole EM-range without any decreasing effectiveness. For metallic composites fluctuations of *SE*-values are quite large. CNTs, however, allow for achieving high *SE*-values, but in some cases, they are lower than those for pristine metal additives. However, the amount of metal (nano)particles is often much higher. It should be decided for a given application if such a high value is necessary (i.e. 20 dB corresponds to attenuation of 90%, 40 dB corresponds to attenuation of 99%). When designing EMI shields, it should also be taken into account that CNTs are much lighter and corrosion-resistant.

Among commercially available RAMs, the range of frequencies 1-18 GHz dominate (**Table 4**). Here, the shielding parameters, as calculated per the sample thickness, are definitely lower than for just EMI shielding materials. On the other hand, as in the case of commercially available EMI shielding materials, fluctuations of shielding parameters are rather high.

Table 4 Commercially available RAMs

Name	Specification	Shielding parameter	Frequency range
Q-Zorb 3000 HP	Special shape magnetic fillers in a polymeric binder	0-2 dB	UHF, L, S
Q-ZORB 2000 HF	Thin magnetically loaded elastomeric sheet	0-30 dB	S, C, X, K_u
RFLS	Sheets produced via dipping lightweight open-celled urethane foam into a resistive solution	0-30 dB	S, C, X, K_u
RFRET	Reticulated foam absorber – urethane-based foam with a well-defined open-cell structure	5-40 dB	S, C, X, K_u
SWAM	Magnetically loaded nitrite rubber	n.d.	L, S, C, X, K_u, K, K_A
K-RAM	Aramid fibres (Kevlar) containing a lossy filler, backed by a carbon fibre laminate	10-20 dB	S, C, X, K_u, K, K_A
MR1	Tuned frequency absorber; thin magnetically loaded sheet; carbonyl Fe powder, polydimethylsiloxane, carbonic acid calcium salt bis(1-methyl-1-phynylethyl)peroxide, magnesium hydroxide	<30 dB	L, S, C, X, K_u, K, K_A
MR2	Cavity resonance absorber; thin magnetically loaded sheet; carbonyl Fe powder, polydimethylsiloxane, carbonic acid calcium salt bis(1-methyl-1-phynylethyl)peroxide, magnesium hydroxide	<25 dB	L, S, C, X, K_u, K
MR3	Surface wave absorber; very highly loaded thin sheet; carbonyl Fe powder, polydimethylsiloxane,	<100 dB/cm	L, S, C, X, K_u, K

	carbonic acid calcium salt bis(1-methyl-1-phynylethyl)peroxide, magnesium hydroxide		
MR5	Low frequency absorber; magnetically loaded sheet	<12 dB/cm	UHF L S
MF1	Reticulated foam absorber; lightweight carbon loaded sheet stock	<45 dB	L S C X K_u
MF2	Lossy foam absorber; lightweight conductive carbon loaded sheet stock	<35 dB	L S C X K_u
MF3	Convoluted foam absorber; lightweight conductive carbon loaded sheet stock	<50 dB	L S C X K_u
MC10 Silicone absorber caulk	Two-part liquid silicone magnetically loaded to be electrically equivalent to the cavity resonance sheet absorber; paste; carbonyl Fe, dimethyl methylhydroge siloxane, dimethylvinyl-termininated dimethyl siloxane, dimethylvinylated silica, tetramethyl tetravinyl cyclotetrasiloxane	<25 dB	L S C X K_u K
Carbon foam	Calcined coke (carbon, graphite, carbon foam, graphitic carbon foam)	>60 dB	UHF L S C X K_u K
MAS-200	Flexible resonant absorber; highly active magnetic filler in polyurethane or silicone	>20 dB	UHF L S C X K_u
MAS-300	Thin, flexible absorber with polyurethane or silicone binder	4-63 dB/cm	UHF L S C X K_u
MF-402 Type CR powder	Iron chrome silicide	20 dB	S C X K_u
MF-500 Urethane	Coated carbonyl Fe-based paint in a proprietary urethane acrylic resin (also available as epoxy and silicone-based formulations)	20 dB	S C X K_u
CRA-18-P	Conical loaded rubber	15-20 dB	C X K_u
KV-RA	Resonating tube consisting from magnetically/electrically loaded neoprene or nitrile rubbers	15 dB	L S C X K_u
KV-CRA-100	Conical loaded rubber	10-20 dB	UHF L S C X
KV-RA-U-14.5-PSA	Resonant absorber; magnetically loaded (with metallic alloy and special ferrite) polyurethane rubber sheets	10-35 dB	K_u
KV-SCA-U-1.5	Polyurethane rubber based on magnetically loaded sheets	5-90 dB/cm	L S C X K_u
KV-SCA-P-PU-4.6	Two-part polyurethane/epoxy based magnetically loaded paint	20-63 dB/cm	S C X
REX RADAR-absorbing mat	Special nylon and conductive fibres and vulcanized nitrile rubber backing	15 dB	C X K_u K K_A V W

For CNT materials, the 8-18 GHz range dominates among the tested ones (**Table 5**), however, CNTs may be also used from low to high frequencies because they hold invariable shielding

parameters in the whole frequency range. It is interesting to note that, due to the unique nature of the CNTs, the latter may be used as RAMs and/or EMI shields [111].

Table 5 Summary of patented RAMs based on CNTs

Frequency range	Matrix	CNTs type	Additive	CNT *OD*/*l* [nm/μm]	CNT [wt.%]	*SE*/*t* [dB mm^{-1}]	Patent
V	epoxy resin, epoxy hardener	MWCNT-COOH	Ferrite, carbonyl iron, fullerenes	10-100/10-100	0.1-5	7-20	RU2570003
X, K_u	chiral poly(Schiff base salt)	CNTs	Co and nickel ferrite	n. d./n. d	10-20	<22	CN105062092
UHF, L	Thermoplastic resin (polyamide resin, polyimide resin)	SWCNTs, MWCNTs	CB	0.5-10/n. d.	1-5	1-12	CN104837926
X, K_u	anionic dispersing agent, epoxy resin or bismaleimide resin	MWCNTs, Ni-SWCNTs	Graphene oxide	6-30/10-50	0.1-1	<20	CN103317734
S, C, X	Polymer binder	MWCNTs	Ferrite, carbonyl iron, fullerene	10-100/10-100	4-5	7-20	RU2482149
X	Epoxy resin, polyurethane, polyethylene, Kevlar, epoxy/phenolic polyester	CNTs	Carbon fiber, glass fiber,	n. d./n. d.	3-6	>25	EP2518434
X, K_u, K	Polymer binder	CNTs	Powdery ferrite (barium hexagonal ferrite alloyed with scandium ions)	n. d./n. d.	0.1-2	<30	RU2380867
X	Epoxy resin	Co-CNTs	-	n. d./n. d.	0.5-4	12-14	CN101289568
UHF, L, S, C, X, K_u	Polymer, coupling agent	MWCNTs, SWCNTs	-	0.4-100/0.01-1000	0.05-20	8-50	CN1791322A

In order to summarize the state-of-the-art in CNT-based RAM composites and hybrid materials, we again present *SE* normalized to thickness (SE_N) as a function of CNT type, aspect ratio and content in the final material for three different frequencies: 8.2, 12.4 and 18 GHz (**Fig. 13**).

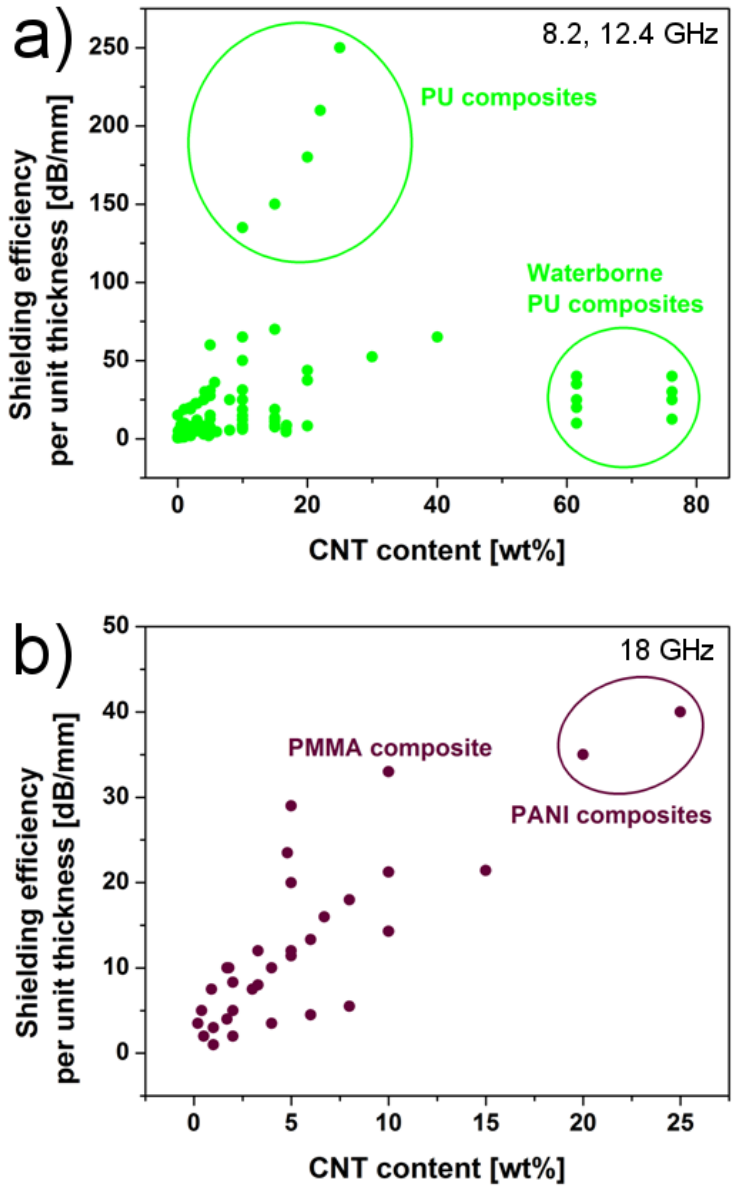

Fig. 13 Shielding efficiency for different CNT composites as a function of CNT content for three frequencies: 8.2 GHz, 12.4 GHz (**a**), 18.0 GHz (**b**)

It can be clearly seen that for 8.2 GHz, the highest *SE* were obtained for the PU-matrix composites. As a filler, MWCNTs of outer diameter 10-50 nm and length 1-10 μm were used. This elevated *SE*-value corresponded to a relatively high MWCNT content (25 wt.%). Similar results were obtained for the 12.4 GHz frequency and 240 dB/mm for MWCNT-PU composite. Moreover, for most of composites it is difficult to correlate *SE*-values with frequencies in the X-range. Slightly different results were obtained for 18 GHz. *SE*-values were generally smaller for all of the composites and the highest recorded *SE*-value was 40 dB mm^{-1}. This value was obtained for MWCNT-PANI composite (MWCNTs of outer diameter

10 nm and length below 10 μm). A high *SE*-value of 31.6 dB mm^{-1} was also found for MWCNT-PMMA composite (MWCNT: diameter = 10 nm, length = 1.5 μm).

7. Conclusions

In the modern world, RAMs and EMI shielding materials are used to control attenuation and absorption of MW, i.e. in aircrafts. For traditional materials, it is difficult to achieve both parameters 'enchanted' in one object, but CNTs make it possible. CNTs – mainly due to high intrinsic electrical conductivity – constitute efficient components in EMI shields and exhibit strong broadband radar-absorbing properties.

A successful manufacture of CNT-based EMI shields and RAMs depends on many factors. Firstly, merging of CNTs and matrix requires high energy mixing as the CNT content required for high *SE*-values is typically far above 10 wt.%. This CNT concentration significantly increases viscosity of the formulation and only full homogenization of the nanofiller may preserve the appreciable mechanical performance. CNT functionalization might here emerge as promising solution, although oxidative treatments may damage their critical electrical, thermal and mechanical properties. Contrarily, surface CNT functionalization allows for tunable compatibilization with polymer and non-polymer matrices. Hence, a compromise, also and mainly because of the economic point-of-view, between CNT content and effectiveness must be undertaken with the help of possible constructional variations of RAMs/EMI shields. A generally beneficial perspective is that shorter and thinner CNTs yield the highest *SE*-values. Fortunately, this type of CNTs is produced in c-CVD processes at the largest industrial scale. For a complete *stealth* action, i.e. at broadest range of working frequencies including masking of the thermal signature of objects, it emerges that universal CNT-based covers must be based on multi-layered structures incorporated into well-defined geometries. Moreover, a dual character of CNT functionalization – encapsulation ferromagnetic NPs in CNTs and exohedral modification of CNTs with conducting NPs or CPs – opens a route to efficient shielding at low CNT content. Nevertheless, the properties-by-design approach requires clear distinguishing between the fates of sent MW-radiation for which lab-scale with theoretical modelling is performed initially but then, inevitably, research in semi-anechoic and anechoic chambers ahead proving grounds are the-must-scenarios.

8. Acknowledgments

The authors are greatly indebted to Silesian University of Technology (BKM-530/RCH2/2016) and The National Centre for Research and Development (TANGO, TANGO1/266702/NCBR/2015), both Poland. D. J. acknowledges National Science Center, Poland (under the Polonez program, grant agreement UMO-2015/19/P/ST5/03799) and the European Union's Horizon 2020 research and innovation programme (Marie Skłodowska-Curie grant agreement 665778).

9. References

1 Machinerieen N. V. Dispositif et procédé pour l'amélioration de dispositifs de production et de réception d'ondes électriques ultra-courtes. FR Patent 802728, 1936.
2 Johnson B. The Secret War. Pen & Sword Military Classics. Barnsley. 2004.
3 Halpern O. Method and means for minimizing reflection of high-frequency radio waves. US Patent 2923934, 1960.
4 Pitkethly MJ. Radar absorbing materials and their potential use in aircraft structures, IEE Colloq. Low Profile Absorbers and Scatterers. London. 1992.
5 Oh JH, Oh KS, Kim CG, Hong CS. Design of radar absorbing structures using glass/epoxy composite containing carbon black in X-band frequency ranges. Compos Part B-Eng 2004; 35:49–56.
6 Al-Saleh MH, Saadeh WH, Sundararaj U. EMI shielding effectiveness of carbon based nanostructured polymeric materials: A comparative study. Carbon 2013; 60:146–156.
7 Popov VN. Carbon nanotubes: properties and application. Mat Sci Eng R 2004; 43:61–102.
8 Saville P. Review of radar absorbing materials. Defence R&D Canada - Atlantic. Dartmouth. 2005.
9 Vinoy KJ, Jha RM. Trends in radar absorbing materials technology. Sadhana 1995; 20:815–850.
10 Ramasamy SR. A review of EMI shielding and suppression materials. Electromagnetic Interference and Compatibility '97. Proceedings of the International Conference on. Hyderabad. December, 1997.
11 Geetha S, Satheesh Kumar KK, Rao ChRK, Vijayan M, Trivedi DC. EMI shielding: methods and materials - a review. J Appl Polym Sci 2009; 112:2073–2086.
12 Lu S, Zeng X, Nie P. Zhang C, Liu C Gao Y et al. Method for preparing radar wave-absorbing composite material based on carbon nanometer film. CN Patent 103317734, 2013.
13 Zhao J, Wang T. RAM made of carbon nano tube and preparation method thereof. CN Patent 1466218, 2004.
14 Chung DDl. Review Electromagnetic interference shielding effectiveness of carbon materials. Carbon, 2001; 39,:279–285.
15 Saini P, Arora M. Microwave absorption and EMI shielding behavior of nanocomposites based on intrinsically conducting polymers, graphene and carbon nanotubes. In: New Polymers for Special Applications, vol 3, Rijeka; 2012 p. 71–112.
16 Zhang S, Jin L, Wu Y, Wu Q, Li LW. A Novel Transparent Carbon Nanotube Film for Radio Frequency Electromagnetic Shielding Applications. Microwave Conference. Singapore. December, 2009.

17 Liu Z, Gang B, Huang Y, Li F, Ma Y, Guo T et al. Microwave Absorption of Single-Walled Carbon Nanotubes/Soluble Cross-Linked Polyurethane Composites. J Phys Chem C 2007; 111:13696–13700.
18 Kumar GS, Vishnupriya D, Joshi A, Datar S, Patro TU. Electromagnetic interference shielding in 1–18 GHz frequency and electrical property correlations in poly(vinylidene fluoride)–multi-walled carbon nanotube composites. Phys Chem Chem Phys2015; 31: 20347-20360.
19 Joshi A, Bajaj A, Singh R, Alegaonkar PS, Balasubramanian K, Datar S. Graphene nanoribbon–PVA composite as EMI shielding material in the X band. Nanotechnology 2013; 24:455705.
20 Aparna AR, Brahmajirao V, Karthikeyan TV. Review on Nano particle synthesis for usage in Nano-Composites for EMI shielding. Int J Innov Res Sci Eng Technol 2013; 2:7391–7401.
21 Abdi MM, Kassim, AB, Ekramul Mahmud HNM, Yunus WMM, Talib ZA. Electrical and shielding properties of conductive polymer composite matrix with chitosan. Solid State Science and Technology 2009; 17:12-21.
22 Farhan S, Wang R, Li K. Electromagnetic interference shielding effectiveness of carbon foam containing in situ grown silicon carbide nanowires. Ceramics International 2016; 9:11330-11340.
23 Chen M, Zhang L, Duan S, Jing S, Jiang H, Luo M et al. Highly conductive and flexible polymer composites with improved mechanical and electromagnetic interference shielding performances. Nanoscale 2014; 6:3796-3803.
24 Ma CCM, Huang YL, Kuan HC, Chiu, YS. Preparation and Electromagnetic Interference Shielding Characteristics of Novel Carbon-Nanotube/Siloxane/Poly-(urea urethane) Nanocomposites . J Polym Sci 2005; 43:345–358.
25 Gao Q, Yin Y, Yan DB, Yuan NC. Application of metamaterials to ultra-thin radar absorbing material design. Electron Lett 2005; 41:936–937.
26 Oraizi H, Abdolali A, Vaseghi N. Application of double zero metamaterials as radar absorbing materials for the reduction of radar cross section. Prog Electromagn Res 2010; 101:323–337.
27 Knott EF. Radar Cross Section. In: Radar Handbook, vol 11, New York and London; 1990 p. 11.1–11.34.
28 Panwar R, Agarwala V, Singh D. A cost effective solution for development of broadband radar absorbing material using electronic waste. Ceram Int 2015; 41:2923–2930.
29 Hammond III HK, Mason HL. Precision Measurement and Calibration Selected NBS Papers on Radiometry and Photometry. National Bureau of Standards. Washington. 1971.
30 Spitalsky Z, Tasis D, Papagelis K, Galiotis C. Carbon nanotube–polymer composites: Chemistry, processing, mechanical and electrical properties. Prog Polym Sci 2010; 35:357–401.
31 Hayashida K, Matsuoka Y. Electromagnetic interference shielding properties of polymer-grafted carbon nanotube composites with high electrical resistance. Carbon 2015; 85:363–371.
32 Udmale V, Mishra D, Gadhave R, Pinjare D, Yamgar R. Development trends in Conductive Nano-Composites for Radiation Shielding. Orient . Chem 2013; 29: 927-936.
33 IIjima S. Helical microtubules of graphitic carbon. Nature 1991; 354:56–58.
34 Radushkevich LV, Lukyanowich VM. O strukture ugleroda, obrazujacegosja pri termiceskom razlozenii okisi ugleroda na zeleznom kontakte. Zurn Fis Chim 1952; 26:88–95.
35 Kaur R, Deep Aul G. Review on Microwave Absorbing Material using
Different Carbon Composites. International Journal of Engineering Research and Technology 2014; 3:160–167.

36 Savi P, Miscuglio M, Giorcelli M, Tagliaferro A. Analysis of Microwave Absorbing Properties of Epoxy MWCNT Composites, PIER Letters 2014; 44:63–69.
37 Che BD, Nguyen BQ, Nguyen LTT, Nguyen HT, Nguyen VQ, Le TV et al. The impact of different multi-walled carbon nanotubes on the X-band microwave absorption of their epoxy nanocomposites. Chem Cent J 2015; 9:1-13.
38 Agel A, Abou El-Nour KMM, Ammar RAA, Al-Wartham A. Carbon nanotubes, science and technology part (I) structure, synthesis and characterisation. Arab J Chem 2012; 5:1–23.
39 Ruoff RS, Qian D, Liu WK. Mechanical properties of carbon nanotubes: theoretical predictions and experimental measurements. C R Physique 2003; 4:993–1008.
40 Agarwal A, Bakshi SR, Lahiri D. Carbon Nanotubes Reinforced Metal Matrix Composites, CRC Press Taylor & Francis Group. Boca Raton. 2011.
41 Chico L, Crspi VH, Benedict LX, Louie SG, Cohen ML. Pure carbon nanoscale devices: nanotube heterojunctions. Phys Rev Lett 1996; 76:971–974.
42 Joselevich E, Dai H., Liu J, Hata K, Windle AH. Carbon Nanotube Synthesis and Organization. In: Topics Appl.Physics, Berlin; 2008 p. 101-164.
43 Jost O, Gorbunov A, Liu X, Pompe W, Fink J. Single-Walled Carbon Nanotube Diameter. J Nanosci Nanotechnol 2004; 4:433-440.
44 Jang SH, Yin H. Effective electrical conductivity of carbon nanotube-polymer composites: a simplified model and its validation. Mater Res Express 2015; 2:045602.
45 Yan KY, Xue QZ, Zheng QB, Hao LZ. The interface effect of the effective electrical conductivity of carbon nanotube composites. Nanotechnology 2007; 18:1-6.
46 Yao Z, Wang JS, Li B, Liu GR. Thermal conduction of carbon nanotubes using molecular dynamics. Phys Rev B 2005; 71:085417.
47 Shiomi J, Maruyama S. Diffusive-Ballistic Heat Conduction of Carbon Nanotubes and Nanographene Ribbons. Int J Thermophys 2010; 31:1945–1951.
48 Zhou Q, Meng F, Liu Z, Shi S. The Thermal Conductivity of Carbon Nanotubes with Defects and Intramolecular Junctions. J Nanomater 2013; 2013:1–7.
49 Schmidt RH, Kinloch IA, Burgess AN, Windle AH. The Effect of Aggregation on the Electrical Conductivity of Spin-Coated Polymer/Carbon Nanotube Composite Films. Langmuir 2007; 23:5707-5712.
50 Kim YY, Yun J, Lee YS, Kim HI. Preparation and Characteristics of Conducting Polymer-Coated MWCNTs as Electromagnetic Interference Shielding Materials. Carbon Lett 2011; 12:48–52.
51 Koledintseva MY. Modelling of shielding composite materials and structures for microwave frequencies. Prog Electromagn Res 2009; 15:197–215.
52 Zhang J, Shi C, Ji T, Wu G, Kou K. Preparation and Microwave Absorbing Characteristics of Multi-Walled Carbon Nanotube/Chiral-Polyaniline Composites. OJPChem 2014; 4:62–72.
53 Xu H, Anlage SM, Hu L, Gruner G. Microwave shielding of transparent and conducting single-walled carbon nanotube films. Appl Phys Lett 2007; 90:90–92.
54 Chung DDL. Carbon materials for structural self-sensing, electromagnetic shielding and thermal interfacing. Carbon 2012; 50:3342–3353.
55 Park SH, Theilmann P, Asbeck P, Bandaru PR. Enhanced electromagnetic interference shielding through the use of functionalized carbon nanotube-reactive polymer composites. IEEE Trans Nanotechnol 2010; 9:464–469.
56 Ji K, Zhao H, Zhang J, Chen J, Dai Z, Fabrication and electromagnetic interference shielding performance of open-cell foam of a Cu–Ni alloy integrated with CNTs. Appl Surf Sci 2014; 311: 351–356.

57 Gui X, Ye W, Wei J, Wang K, Lv R, Zhu H et al. Optimization of electromagnetic matching of Fe-filled carbon nanotubes/ferrite composites for microwave absorption. J Phys D Appl Phys 2009; 42:075002.
58 Micheli D, Pastore R, Vricella A, Morles RB, Marchetti M, Delfini A et al. Electromagnetic characterization and shielding effectiveness of concrete composite reinforced with carbon nanotubes in the mobile phones frequency band. Mater Sci Eng B 2014; 188:119–129.
59 BJ, Bae KM, Lee YS, An KH, Park SJ. EMI shielding behaviors of Ni-coated MWCNTs-filled epoxy matrix nanocomposites. Surf Coat Tech 2014; 242:125–131.
60 Im JS, Park IJ, In SJ, Kim T, Lee YS. Fluorination effects of MWCNT additives for EMI shielding efficiency by developed conductive network in epoxy complex. J Fluorine Chem 2009; 130:1111–1116.
61 Yuen SM, Ma CCM, Chuang CY, Yu KC, Wu SY, Yang CC et al. Effect of processing method on the shielding effectiveness of electromagnetic interference of MWCNT/PMMA composites. Compos Sci and Technol 2008; 68:963–968.
62 Kim HM, Kim K, Lee SJ, Joo J, Yoon HS, Cho SJ et al. Charge transport properties of composites of multiwalled carbon nanotube with metal catalyst and polymer: application to electromagnetic interference shielding. Curr Appl Phys 2004; 4:577–580.
63 Yim YJ, Park SJ. Electromagnetic interference shielding effectiveness of high-density polyethylene composites reinforced with multi-walled carbon nanotubes. J Ind Eng Chem 2015; 21:155–157.
64 Jou WS, Cheng HZ, Hsu CF. The electromagnetic shielding effectiveness of carbon nanotubes polymer composites. J Alloy Compd 2007; 434–435:641–645.
65 Huang Y, Li N, Ma Y, Du F, Li F, He X et al. The electromagnetic shielding effectiveness of carbon nanotubes polymer composites. Carbon 2007; 45:1614–1621.
66 Pha CH, Mariatti M, Koh YH. Electromagnetic interference shielding performance of epoxy composites filled with multiwalled carbon nanotubes/manganese zinc ferrite hybrid fillers. J Magn Magn Mater. 2016; 401:472–478.
67 Liu Y, Song D, Wu C, Leng J. EMI shielding performance of nanocomposites with MWCNTs, nanosized Fe_3O_4 and Fe. Compos Part B Eng 2014; 63:34–40.
68 Zeng Z, Chen M, Jin H, Li W, Xue X, Zhou L et al. Thin and flexible multi-walled carbon nanotube/waterborne polyurethane composites with high-performance electromagnetic interference shielding. Carbon 2016; 96:768–777.
69 Gupta TK, Singh BP, Dhakate SR, Singh VN, Mathur RB. Improved nanoindentation and microwave shielding properties of modified MWCNT reinforced polyurethane composites. J Mater Chem A 2013; 32:9138–9149.
70 Liu Z, Bai G, Huang Y, Ma Y, Du F, Li F et al. Reflection and absorption contributions to the electromagnetic interference shielding of single-walled carbon nanotube/polyurethane composites. Carbon 2007; 45:821–837.
71 Hoang AS. Electrical conductivity and electromagnetic interference shielding characteristics of multiwalled carbon nanotube filled polyurethane composite films. Adv Nat Sci Nanosci Nanotechnol 2011; 2:025007.
72 Joseph N, Janardhanan C, Sebastian MT. Electromagnetic interference shielding properties of butyl rubber-single walled carbon nanotube composites. Compos Sci Technol 2014; 101:139–144.
73 Chen M, Yin X, Li M, Chen L, Cheng L, Zhang L. Electromagnetic interference shielding properties of silicon nitride ceramics reinforced by in situ grown carbon nanotubes. Ceram Int 2015; 41:2467–2475.

74 Huang YL, Yuen SM, Ma CCM, Chuang CY, Yu KC, Teng CC et al. Morphological, electrical, electromagnetic interference (EMI) shielding, and tribological properties of functionalized multi-walled carbon nanotube/poly methyl methacrylate (PMMA) composites. Compos Sci Technol 2009; 69:1991–1996.
75 Verma P, Saini P, Choudhary V. Designing of carbon nanotube/polymer composites using melt recirculation approach: Effect of aspect ratio on mechanical, electrical and EMI shielding response. Mater Design 2015; 88:269–277.
76 Singh AP, Gupta BK, Mishra M, Govind, Chandra A, Mathur RB et al. Multiwalled carbon nanotube/cement composites with exceptional electromagnetic interference shielding properties. Carbon 2013; 56:86–96.
77 Li Y, Chen C, Zhang S, Ni Y, Huang J. Electrical conductivity and electromagnetic interference shielding characteristics of multiwalled carbon nanotube filled polyacrylate composite films. Appl Surf Sci 2008; 254:5766–5771.
78 Theilmann P, Yun SJ, Asbeck P, Park SH. Superior electromagnetic interference shielding and dielectric properties of carbon nanotube composites through the use of high aspect ratio CNTs and three-roll milling. Org Electron 2013; 14:1531–1537.
79 Al-Saleh MH. Influence of conductive network structure on the EMI shielding and electrical percolation of carbon nanotube/polymer nanocomposites. Synt Met 2015; 205:78–84.
80 Qing Y, Mu Y, Zhou Y, Luo F, Zhu D, Zhou W. Multiwalled carbon nanotubes–$BaTiO_3$/silica composites with high complex permittivity and improved electromagnetic interference shielding at elevated temperature. J Eur Ceram Soc 2014; 34:2229–2237.
81 Gupta A, Choudhary V. Electromagnetic interference shielding behavior of poly(trimethylene terephthalate)/multi-walled carbon nanotube composites. Compos Sci Technol 2011; 71:1563–1568.
82 Saini P, Choudhary V, Singh BP, Mathur RB, Shawan SK. Polyaniline–MWCNT nanocomposites for microwave absorption and EMI shielding. Mater Chem Phys 2009; 113:919–926.
83 Verma P, Saini P, Malik RS, Choudhary V. Excellent electromagnetic interference shielding and mechanical properties of high loading carbon-nanotubes/polymer composites designed using melt recirculation equipped twin-screw extruder. Carbon 2015; 89:308–317.
84 Zhang CS, Ni QQ, Fu SY, Kurashiki K. Electromagnetic interference shielding effect of nanocomposites with carbon nanotube and shape memory polymer. Compos Sci Technol 2007; 67:2973–2980.
85 Xiang C, Pan Y, Guo J. Electromagnetic interference shielding effectiveness of multiwalled carbon nanotube reinforced fused silica composites. Ceram Int 2007; 33:1293–1297.
86 Zhao DL, Li X, Shen ZM. Preparation and electromagnetic and microwave absorbing properties of Fe-filled carbon nanotubes. J Alloy Comp 2009; 471:457–460.
87 Lin H, Zhu H, Guo H, Yu L. Investigation of the microwave-absorbing properties of Fe-filled carbon nanotubes. Mat Lett 2007; 61:3547–3550.
88 Kim HM, Kim K, Lee CY, Joo J. Electrical conductivity and electromagnetic interference shielding of multiwalled carbon nanotube composites containing Fe catalyst. Appl Phys Lett 2004; 84:589–591.
89 Lin H, Zhu H, Guo H, Yu L. Microwave-absorbing properties of Co-filled carbon nanotubes. Mater Res Bull 2008; 43:2697–2702.
90 Kim BJ, Bae KM, Seo MK, An KH, Park SJ. Roles of Ni/CNTs hybridization on rheological and mechanical properties of CNTs/epoxy nanocomposites. Mater Sci Eng A 2011; 528:4953–4957.

91 Kwon S, Ma R, Kim U, Choi HR, Baik S. Flexible electromagnetic interference shields made of silver flakes, carbon nanotubes and nitrile butadiene rubber. Carbon 2014; 68:118–124.
92 Zhao DL, Li X, Shen ZM. Electromagnetic and microwave absorbing properties of multi-walled carbon nanotubes filled with Ag nanowires. Mater Sci Eng B 2008; 150:105–110.
93 Song WL, Cao MS, Wen B, Hou ZL, Cheng J, Yuan J. Synthesis of zinc oxide particles coated multiwalled carbon nanotubes: Dielectric properties, electromagnetic interference shielding and microwave absorption. Mater Res Bull 2012; 47:1747–1754.
94 Kong L, Yin X, Han M, Zhang L, Cheng L. Carbon nanotubes modified with ZnO nanoparticles: High-efficiency electromagnetic wave absorption at high-temperatures. Ceram Int 2015; 41:4906–4915.
95 M Arjmand M, Sundararaj U. Electromagnetic interference shielding of Nitrogen-doped and Undoped carbon nanotube/polyvinylidene fluoride nanocomposites: A comparative study. Compos Sci Technol 2015; 118:257–263.
96 Silva VA, de Castro Folgueras L, Candido GM, de Paula AL, Rezende MC, Costa ML. Nanostructured composites based on carbon nanotubes and epoxy resin for use as radar absorbing materials . Mater Res 2013; 16:1299–1308.
97 Zakharychev EA, Kabina MA, Razov EN, Svetlakov YA, Istomin LA. Effect of functionalization of carbon nanotubes on the radar-absorbing properties of polymeric composites based on them. Russ J Appl Chem 2015; 88:302–307.
98 Ren F, Yu H, Wang L, Sallem M, Tian Z, Ren P. Current progress on the modification of carbon nanotubes and their application in electromagnetic wave absorption. RSC Adv 2014; 4:14419–14431.
99 Liu R, Zhao Z, Miao X, Cao Y. Anti-radar coating and preparation method thereof. CN Patent 102807801, 2012.
100 Liu Z, Bai G, Huang Y, Li F, Ma Y, Guo T et al. Microwave Absorption of Single-Walled Carbon Nanotubes/Soluble Cross-Linked Polyurethane Composites. J Phys Chem C 2007; 111:13696–13700.
101 Dinesh P, Renukappa NM, Siddaramaiah, Rajan S. Electrical Resistivity and Electromagnetic Interference Shielding Effectiveness of Multiwalled Carbon Nanotubes filled Carbon Black-High Density Polyethylene Nanocomposites. International Conference on Electronics, Biomedical Engineering and its Applications. Dubai. January, 2012.
102 Zhao T, Hou C, Zhang H, Zhu R, She S, Wang J et al. Electromagnetic Wave Absorbing Properties of Amorphous Carbon Nanotubes. Sci Rep 2014; 4:5619.
103 Kim YY, Yun J, Lee YS, Kim HI. Preparation and Characteristics of Conducting Polymer-Coated MWCNTs as Electromagnetic Interference Shielding Materials. Carbon Lett 2011; 12:48–52.
104 Makeiff DA, Huber T. Microwave absorption by polyaniline–carbon nanotube composites. Synthetic Met 2006; 156:497–505.
105 Zhang W, Xiong H, Wang S, Li M, Gu Y. Electromagnetic characteristics of carbon nanotube film materials. Chin J Aeronaut 2015; 28:1245–1254.
106 Arjmand M, Apperley T, Okoniewski M, Sundararaj U. Comparative study of electromagnetic interference shielding properties of injection molded versus compression molded multi-walled carbon nanotube/polystyrene composites. Carbon 2012; 50:5126-5134.
107 Yuan B, Yu L, Sheng L, An K, Zhao X. Comparison of electromagnetic interference shielding properties between single-wall carbon nanotube and graphene sheet/polyaniline composites. J Phys D Appl Phys 2012; 45:235108.

108 Gupta TK, Singh BP, Mathur RB, Dhakate SR. Multi-walled carbon nanotube–graphene–polyaniline multiphase nanocomposite with superior electromagnetic shielding effectiveness. Nanoscale 2014; 6:842–851.
109 Ting TH, Jau YN, Yu RP. Microwave absorbing properties of polyaniline/multi-walled carbon nanotube composites with various polyaniline contents. Appl Surf Sci 2012; 258:3184–3190.
110 David T, Mathad JK, Padmavathi T, Vanaja A. Part-A: Synthesis of polyaniline and carboxylic acid functionalized SWCNT composites for electromagnetic interference shielding coatings. Polymer 2014; 55:5665–5672.
111 Li CY. Composite material with electromagnetic shielding and radar wave-absorbing function and preparing method. CN Patent 1791322, 2006.